OSSERVATORIO ASTROFISICO DI CATANIA

Characterization of the recently manufactured LCT5 and LVR Hamamatsu SiPMs suitable for the pre-production telescopes

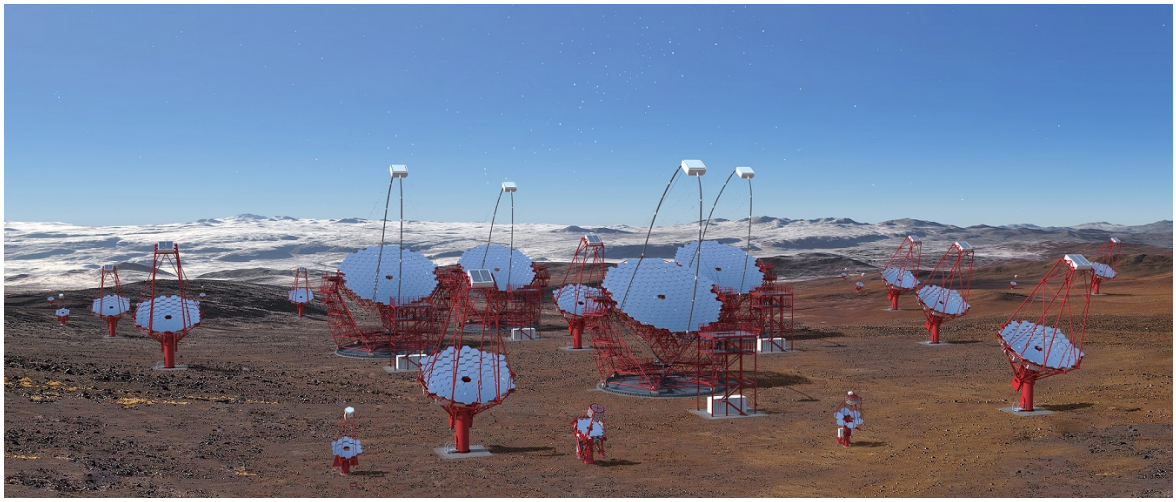

Osservatorio Astrofisico di Catania

G.Romeo(1), G.Bonanno(1)

(1) INAF – Osservatorio Astrofisico di Catania

Rapporti interni e tecnici
N.2/2017

INDEX

LIST OF ACRONYMS

OACT	Osservatorio Astrofisico di Catania
IFC	Istituto di Astrofisica Spaziale e Fisica Cosmica di Palermo
COLD	Catania astrophysical Observatory Laboratory for Detectors
PCB	Printed Circuit Board
SiPM	Silicon Photo-Multiplier
MPPC	Multi Pixel Photon Counter
SST-2M	Small-Size Telescope Dual-Mirror
PDM	Photon Detection Module
ASIC	Application Specific Integrated Circuit
FEE	Front-End Electronics
BEE	Back-End Electronics
FPGA	Field Programmable Gate Array
EASIROC	Extended Analogue Silicon-pm Integrated Read-Out Chip
CITIROC	Cherenkov Imaging Telescope Integrated Read-Out Chip
I/F	Interface
LCT	Low Cross Talk
PSAU	Power Supply and Amplification Unit
PDE	Photon Detection Efficiency
SCA	Switched Capacitor Array
OCT	Optical Cross Talk
LVR	Low Voltage Resistor
LVR2	Low Voltage Resistor 2nd Version
PHD	Pulse Height Distribution

1. INTRODUCTION

The Cherenkov Telescope Array (CTA) will be the largest ground-based observatory operating in the very-high-energy gamma-ray (20 GeV –300 TeV) range. It will be based on more than one hundred telescopes, located in two sites (in the northern and southernhemispheres). The energy coverage, in the southern CTA array, will extend up to hundreds of TeV thanks to a large number (up to 70) of small size telescopes, with their primary mirrors of about 4 meters in diameter and large field of view of the order of 9 degrees. It is proposed that one of the first sets of precursors for the CTA small size telescope arrays will be represented by the ASTRI mini-array which includes (at least) nine ASTRI telescopes.

ASTRItelescopes are characterized by adual-mirror optical design based on the Schwarzschild-Couder (SC) configuration. The focal-plane camera is curved in order to fit the ideal prescription for the SC design and the sensors are small size silicon photomultipliers managed by a fast front-end electronics.

The need to select the most suitable detectors to cover the ASTRI-Mini Array telescopes focal plane, and the need to be compliant in terms of methodology and techniques with other research laboratories, included Hamamatsu Photonics, has brought us to develop a new characterization technique to study the main features of the recently available SiPMs manufactured by Hamamatsu. In fact big progress have been achieved to improve the relevant SiPM characteristics such us the Photon Detection Efficiency (PDE) and the Optical Cross Talk (OCT).

This document illustrates the experimental setup developed to measure and characterize the SiPM detectors.

These measurements include:

- PDE in the spectral range of 300-1000 nm by using pulsed light sources
- PDE @405nm versus overvoltage
- OCT and Dark Count Rate (DCR) versus overvoltage

As stated above, these last are carried out on the recently available SiPM devices manufactured by Hamamatsu Photonics. They are different in size and in technology. In particular, this report presents the results on the following SiPMs:

- ***LCT5 3050CS*** **3 × 3** mm^2 with microcell **50** µm Silicone Coated
- ***LCT5 7050CS*** **7 × 7** mm^2 with microcell **50** µm Silicone Coated
- ***LCT5 3075CS*** **3 × 3** mm^2 with microcell **75** µm Silicone Coated
- ***LCT5 6075CS*** **6 × 6** mm^2 with microcell **75** µm Silicone Coated
- ***LCT5 7075CS*** **7 × 7** mm^2 with microcell **75** µm Silicone Coated
- ***LVR 3050CS*** **3 × 3** mm^2 with microcell **50** µm Silicone Coated
- ***LVR2 3050CN*** **3 × 3** mm^2 with microcell **50** µm Not Coated (Bare)
- ***LVR2 7050CS*** **7 × 7** mm^2 with microcell **50** µm Silicone Coated
- ***LVR2 7050CN*** **7 × 7** mm^2 with microcell **50** µm Not Coated (Bare)

We focused a particular attention to the SiPMs of size of 7 x 7 mm^2.because they are the ones forming the individual Photon Detection Module (PDM).

2. Characterization Setup

We schematized the adopted setup in Figure 1. The apparatus allows PDE measurements in the spectral range of 300 - 1000 nm by using 18 pulsed light sources. The wavelength of each source is reported in Table 1 of paragraph 2.1. Furthermore, we use the same setup to measure PDE, OCT and DCR versus Overvoltage.

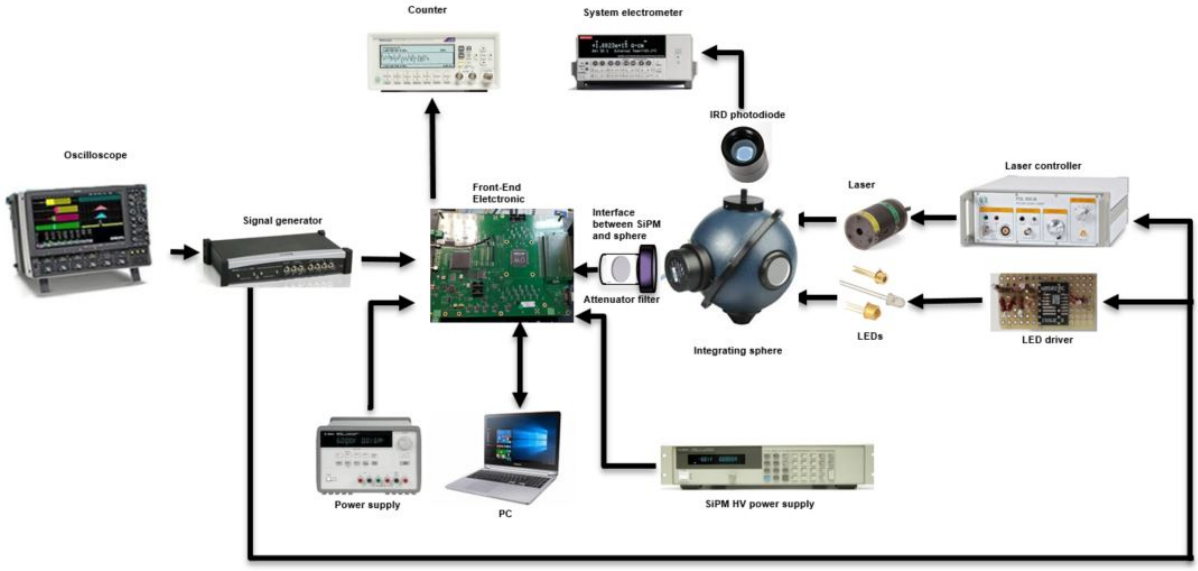

Figure 1. Characterization setup based on the use of pulsed light sources: Lasers and LEDs

The system is constituted by:

- Power supply Agilent 6634B
  (to supply the high voltage to the SiPM)
- Power supply Agilent E3631A
  (to supply the voltage levels to the LED driver)
- Counter Tektronics FCA 3000
  (to measure the count rate for the stairs case)
- Electrometer System Keithley 6514
  (to measure the photo-current form the reference detector)
- Calibrated Photodiode IRD NIST traceable
  (to detect the luminous flux inside the integrating sphere)
- Oscilloscope LeCroy wavePro 725Zi 2.5GHz
  (to process synchro signals for the pulsed light source)
- Pulse generator LeCroy ArbStudio 1104
  (to generate synchro signals for the pulsed light source)
- LEDs Driver
  (see section 2.2)
- Pulsed diode laser controller PicoQuant PDL 200-B
  (to drive the lasers)
- Integrating sphere Labsphere
  (to obtain a uniform light flux on detectors surface)
- Front-end electronics based on the CITIROC 1A
  (to process the SiPM signals see section 2.4)
- Temperature sensor LMT70 and controller ADAM 4017
  (to control the SiPM temperature in order to compensate the power supply voltage to maintain constant the SiPM gain)
- 16 LED pulsed sources and 3 LASER pulsed sources
  (see Table 1 section 2.1)
- Calibrated neutral filters Thorlabs ND30B, ND20B, ND13B and ND10B
  (see Table 2 section 2.3)

2.1 Pulsed light sources available at the COLD laboratory

The pulsed light sources available at the COLD lab are in total 19 of which 16 LED sources and 3 Laser sources. Table 1 lists the sources and their respective wavelength:

Table 1 – Lists of pulsed light sources: LED and LASER and their respective wavelength

Identifier code	Wavelength [nm]	Type
LDH-P-C-405	405	Laser
EPL-450	450	Laser
LDH-P-635	635	Laser
LED285W	285	LED
LED315W	315	LED
LED341W	341	LED
LED385L	385	LED
LED430L	430	LED
LED450L	450	LED
LED465E	465	LED
PLS-8-2-746	496	LED
LED505L	505	LED
LED525L	525	LED
LED570L	570	LED
LED591E	591	LED
LED660L	660	LED
LED680L	680	LED
LED780E	780	LED
LED851L	851	LED

2.2 LED Driver

To drive the LED sources, we designed and built an appropriate electronic circuit for fast signals. The schematic is depicted in Figure 2.

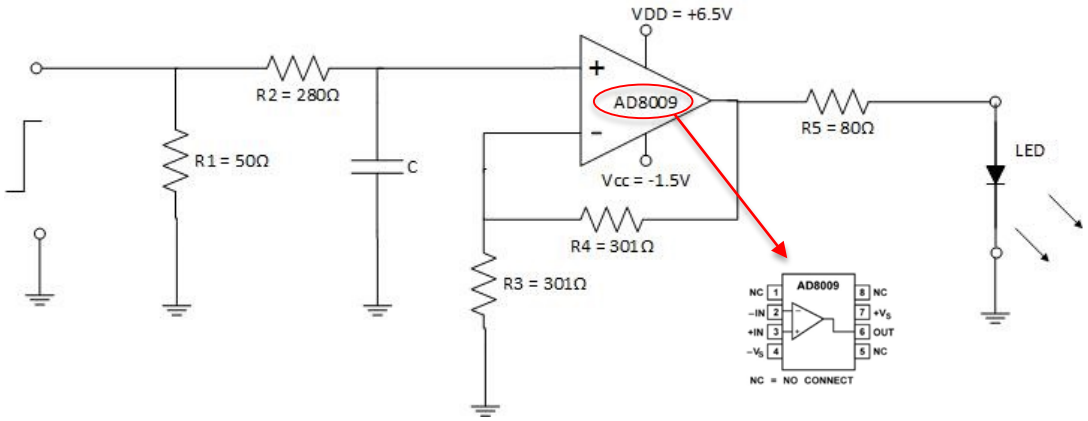

Figure 2. LED driver schematics

The circuit is based on the AD8009 ultra-fast amplifier in non-inverting configuration, capable of conditioning signals at a slew rate of 5.5V/μs (545ps rise time). These features make it ideal as a pulse amplifier.
The AD8009 is characterized by a 440MHz bandwidth at gain G = 2, and is also capable of delivering more than 175mA of load current, while maintaining a low differential gain and a reduced phase error. It is powered with a dual voltage of VDD = + 6.5V and VCC = -1.5V.
In the specific case, the gain was set to 2 by means of the two feedback resistors.
At the input, a coupling resistance (R1) interfaces the signal coming by the function generator whose amplitude is suitably modulated to vary the LED intensity.
The signal is represented by the waveform (blue color) shown in Figure 3. A detailed description of the signals is reported in section 2.4.2.

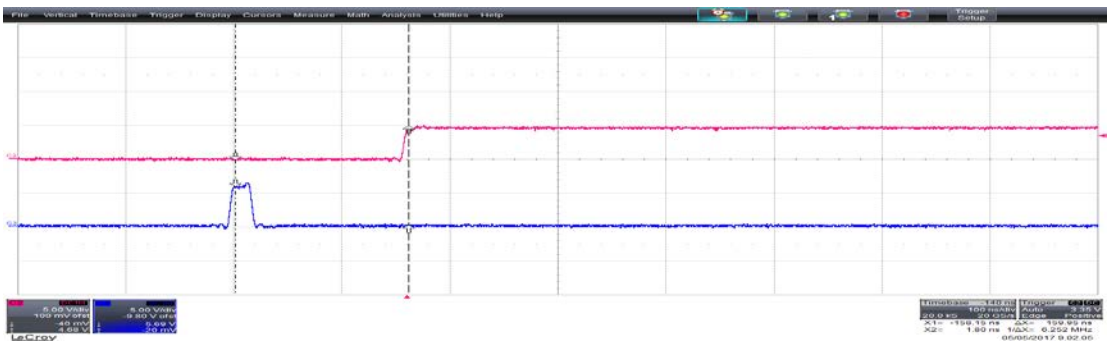

Figure 3. Input signal for the LED driver (waveform blue color) and synchro signal (waveform red color) named HOLD.

In Figure 3, in addition to the signal transmitted to the LED driver (blue waveform), the sync signal (HOLD) is present; this signal is described in section 3.

Specifically, each LED has an appropriate polarization voltage, which is settled at levels to have a suitable photon flux inside the integrating sphere. We recall that for the correct PDE measurements the system must work in single photon counting regime.

2.3 Neutral density filters: type and calibration

To avoid working with luminous level that could saturate the SiPM (degrading the PDE) and at the same time have sufficient current signal detected by the photodiode, we consider mandatory the reduction of the photon flux on SiPM by introducing optical attenuators. These last are neutral filters of different optical transmittance.

For this purpose, we calibrated with high accuracy each single filter to determine the transmittance value according to the correspondent wavelength.

The set-up used for calibrating the filters is shown in the diagram of Figure 4.

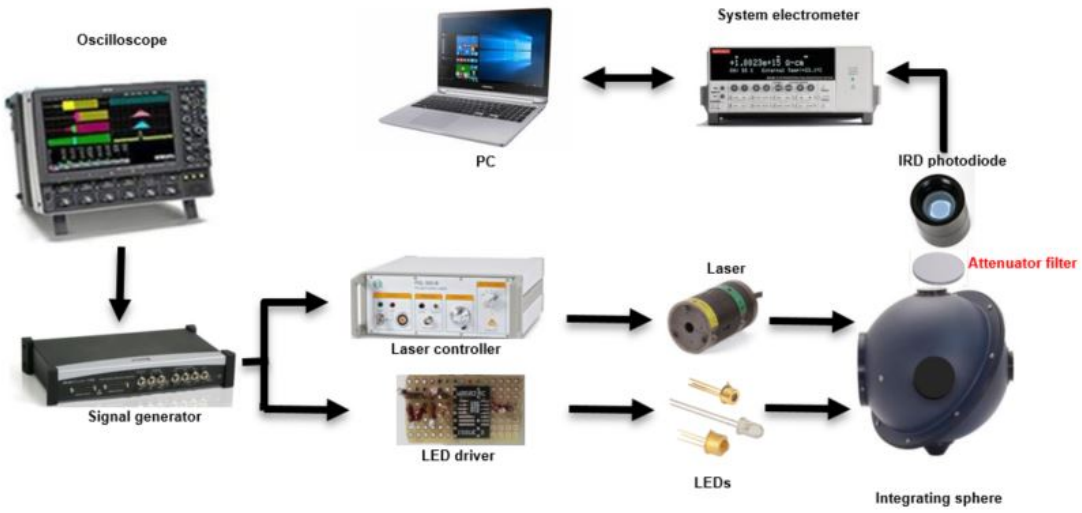

Figure 4. Set-up for calibrating the neutral density filters.

We repeated each single measurement in different light intensity conditions changing both the voltage level and the frequency of the source and alternated the acquisition cycle on a run of 100 measurements of the photocurrent four times with and without the introduction of the attenuator filter to be calibrated. The standard deviation for each set of measurements resulted less than 1%. The final transmittance value is given by the arithmetic mean of the four measurements.

The calibrated neutral density filters are:
ND30B, ND20B, ND13B e ND10B from Thorlabs.

Table 2 shows the result of measurements in terms of transmittance.
In addition, the third column shows Quantum Efficiency of the IRD photodiode whose values are NIST traceable.

Table 2 – Neutral density Filters transmittance and IRD photodiode Quantum Efficiency

FILTER TRANSMITTANCE ND30B,ND20B, ND13B , ND10B and Quantum Efficiency IRD 00-2#-29						
s/n	λ[nm]	QE	ND30B (0,1%)	ND20B (1%)	ND13B (5%)	ND10B (10%)
LED285W	285	0,33114	low signal	0,00676	0,05662	0,06449
LED315W	315	0,44331	low signal	0,00871	0,07320	0,12312
LED341W	341	0,45585	low signal	0,00878	0,07191	0,12667
LED385L	385	0,48872	0,00040	0,00892	0,06840	0,12307
LDH-P-C-405	405	0,53500	0,00042	0,00893	0,06682	0,12054
LED430L	430	0,56975	0,00047	0,00887	0,06472	0,11887
LED450L	450	0,59105	0,00054	0,00917	0,06321	0,11819
EPL-450	450	0,59105	0,00051	0,00911	0,06396	0,11812
LED465E	465	0,60209	0,00057	0,00942	0,06294	0,11713
PLS-8-2-746	496	0,61580	0,00069	0,01007	0,06296	0,11778
LED505L	505	0,62327	0,00077	0,01021	0,06248	0,11694
LED525L	525	0,63422	0,00081	0,01054	0,06246	0,11799
LED570L	570	0,65435	0,00101	0,01144	0,06241	0,11851
LED591E	591	0,64810	0,00106	0,01172	0,06251	0,11811
LDH-P-635	635	0,65620	0,00132	0,01274	0,06295	0,12002
LED660L	660	0,66009	0,00144	0,01319	0,06291	0,12080
LED680L	680	0,65600	0,00161	0,01375	0,06367	0,12209
LED780E	780	0,60844	0,00226	0,01597	0,06577	0,12662
LED851L	851	0,48355	0,00274	0,01726	0,06689	0,12881

For the ND30B filter, it is impossible to evaluate the transmittance for the first three wavelengths (285nm, 315nm, 341nm) due to the low detected signal compared to the signal without filter.

2.4 Front-End Electronics used in the set-up

As electronics front-end, adopted the same used by the ASTRI Mini Array project based on the ASIC chip CITIROC 1A from WEEROC. Here we describe only the circuits involved in the evaluation of the PDE and in general in the SiPM detectors characterization.
The analog core of the chip has 32 channels that incorporate:

- An analog-to-digital converter (ADC) for the SiPM high voltage adjustment.
- Two preamps that allow settling dynamic range, through variable capacitors, between 160fC and 320pC.
- A trigger line consisting of two fast shapers and two discriminators.
- Two slow shapers and two track and hold blocks are responsible for measurement of the charge and then of the Pulse Height Distribution (PHD).

Figure 5 shows the block diagram of one channel.

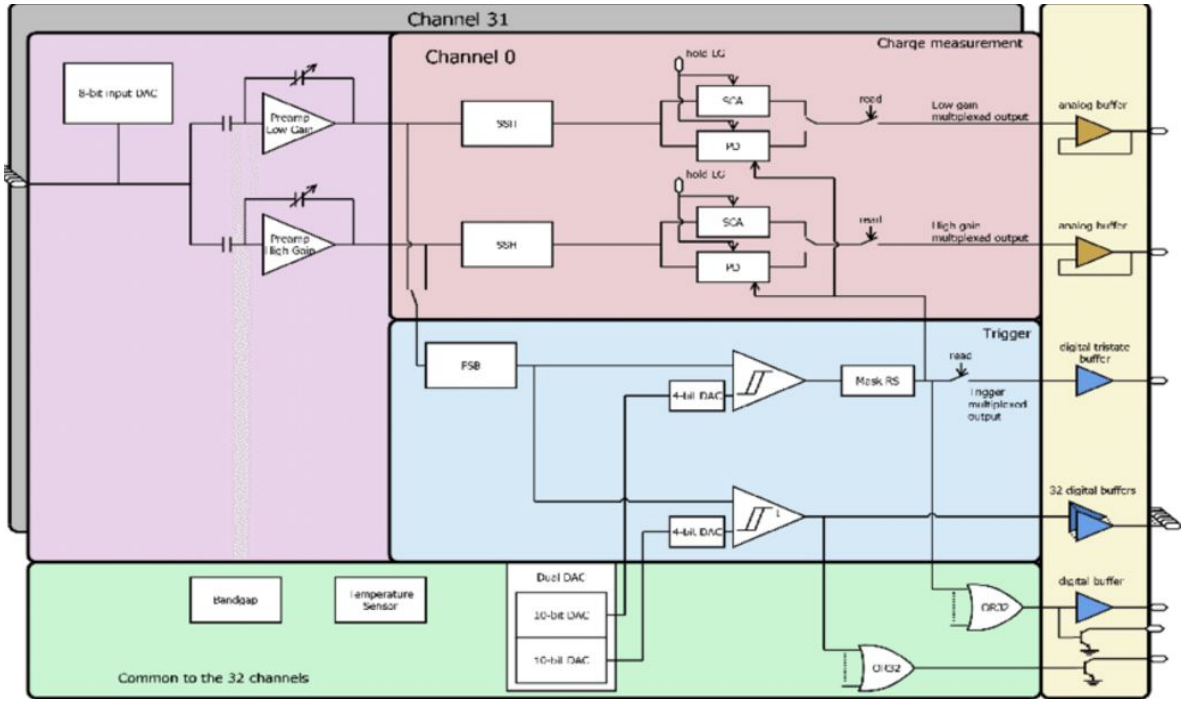

Figure 5. A single channel block diagram of the CITIROC

2.4.1 Optical Cross Talk evaluation through Dark Stairs measurements

The CITIROC part used to obtain staircase measurements is depicted in Figure 6. The SiPM pulse is amplified by the High Gain (HG) preamplifier and then is shaped (15ns shaping time) by the ***Bipolar Fast Shaper***. A discriminator with a programmable threshold (10 bit DAC) is used to drive the output signal through the OR32, and in turn, drive the counter Tektronics FCA 3000.

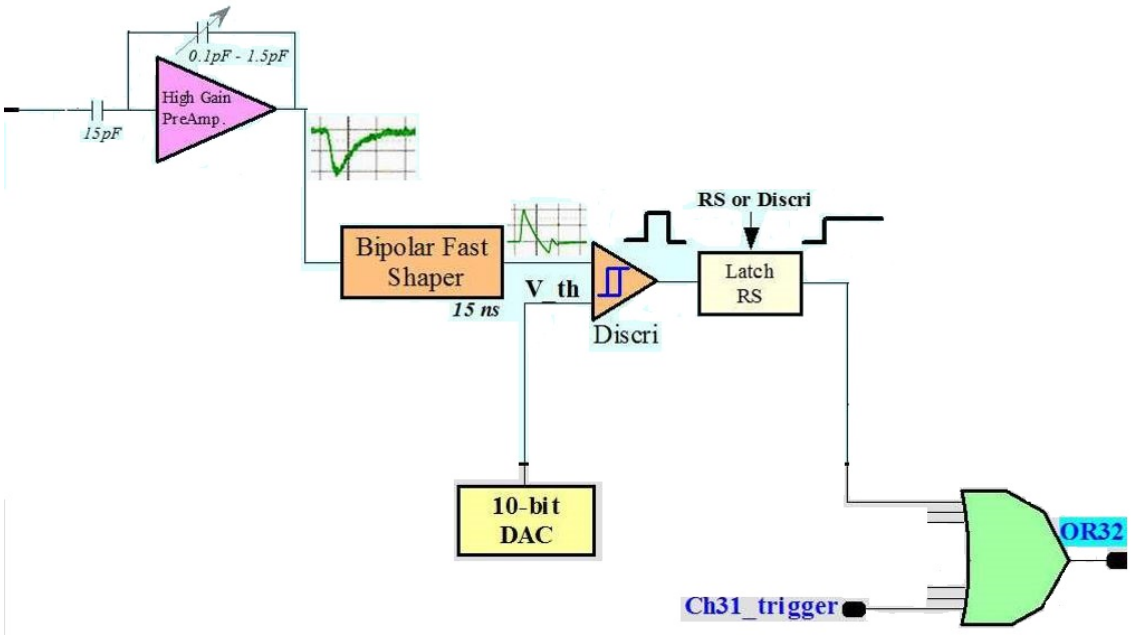

Figure 6. Block diagram of the used electronics inside the ASIC for staircase measurements.

The adopted method essentially consists in measuring the trigger rate as a function of the discriminator threshold in dark condition. Usually data are accumulated in 70 seconds. The result for a particular SiPM detector, the MPPC LVR2 3050CN, is shown in the Figure 7, where the characteristic staircase function is represented: the count rate drops every time integer multiples of 1 p.e. are reached.
The rate of the first plateau, that is relative to discriminator thresholds < 1p.e., gives the total dark count rate, that in the specific case is about 285KCnts/s.
Assuming a Poisson distribution, the probability to have two coincident events within a time window of 15ns is about 10^{-2}% (rate 100 Hz), negligible with respect to the dark rate measured.

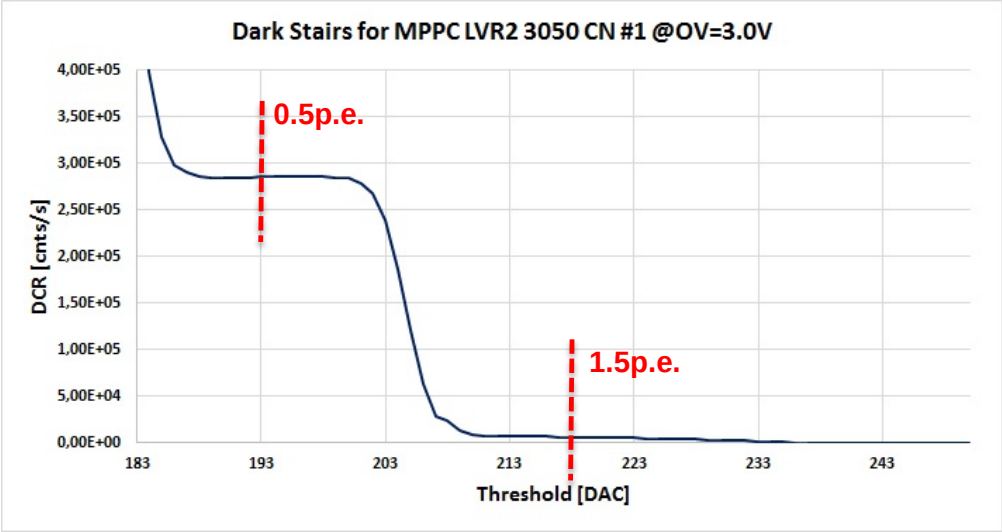

Figure 7. Dark Stairs measured for the MPPC LVR2 3050 CN at 3.0V of overvoltage.

The Optical Cross Talk (OCT) level is evaluated from the ratio between values of DCR[0.5pe] and DCR[1.5pe] as indicated by the formula (1) and marked in the Figure 7 with the red arrows.

$$OCT = \frac{DCR[1.5\ p.e.]}{DCR[0.5\ p.e.]} \quad (1)$$

For the specific case of the MPPC LVR2 3050CN, being the DCR 5,78x10^3 Cnts/s at 1.5p.e. and 2,85x10^5 Cnts/s at 0.5p.e., by applying the formula (1) an OCT of ~ 2% is obtained.

2.4.2 Pulse Height Distribution measurement for the PDE evaluation

The CITIROC part used to obtain Pulse Height Distribution (PHD) measurements is shown in Figure 8.

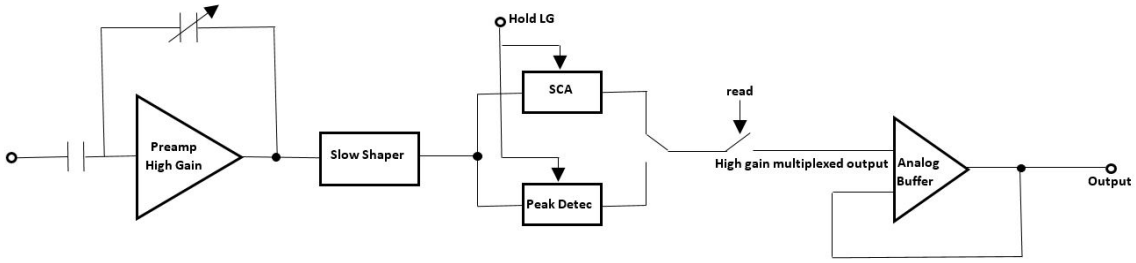

Figure 8. Schematic of the electronics used to measure the Pulse Height Distribution.

In this case the SiPM pulse is amplified by the High Gain (HG) preamplifier and is shaped by the ***Slow Shaper*** that provides a charge measurement. The peaking time can be tuned thanks to the slow control parameters. Seven CRRC shaping times (from 12.5 ns to 87.5 ns) are available

for this ***Slow Shaper***. The selected "peaking time" for our experiments is **37.5 ns**. The amplitude of the pre-amplified and shaped signal at its peaking time is saved by using a track and hold cell. The hold control signal is directly provided to the ASIC by the user on a dedicated pin (***Holdb)***. The selected "Holdb" time for our experiments is **120.0 ns**. Analogue data is stored at the same time on the Switched Capacitor Array (SCA). The read register through the signal "***Read***" controls the readout of this analogue memory. The selected "Read" time for our experiments is **10 µs**.
Figure 9 shows the schematic of the Track and Hold module while Figure 10 shows the standard working mode.

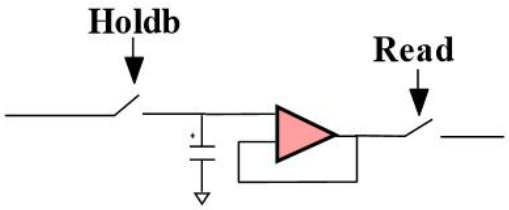

Figure 9. Schematic of track and hold cell.

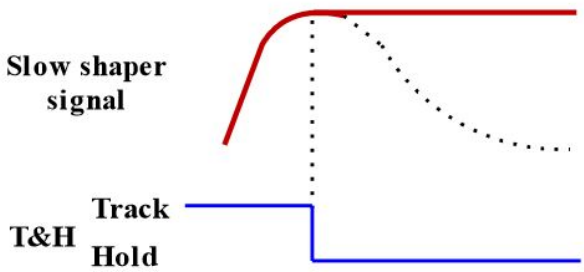

Figure 10. Standard Track and Hold working mode.

In parallel of standard track and hold, Weeroc (under suggestion of INAF) has implemented a peak detector to store the analogue data. The peak detector is controlled by 3 digital signals. These signals are "THb", "Trig" and "Rstb". When nothing happens, the peak detector is in track mode: it works like a voltage follower. When a signal is detected on the trigger channel, the peak detector receives the "Trig" signal and it becomes a real peak detector.
This last operation mode results incompatible with the real measurements of the pedestal because the peak detector module introduces a random offset. For this reason for the PDE measurements, we decide to use only the SCA mode.
In conclusion, the signals used to acquire the pulse height distribution are the HOLD to control the Track and Hold cell and the TRIGGER to control the pulsed light source generator. The Pulse generator LeCroy ArbStudio 1104 generates both signals to drive the entire acquisition process. The HOLD signal has to be delayed with respect to the TRIGGER signal of additional 40ns as the LASER controller and the LED driver need 40ns to generate the flashlight.
This gives a total HOLD time of 160ns respect to the TRIGGER signal. Figure 11 shows the two signals: in the panel a) the 160 ns delay is evident, while panel b) shows the duration of 10 ms of the "Read" signal, finally panel c) shows *the 10 KHz or 10000 pulses/s.*

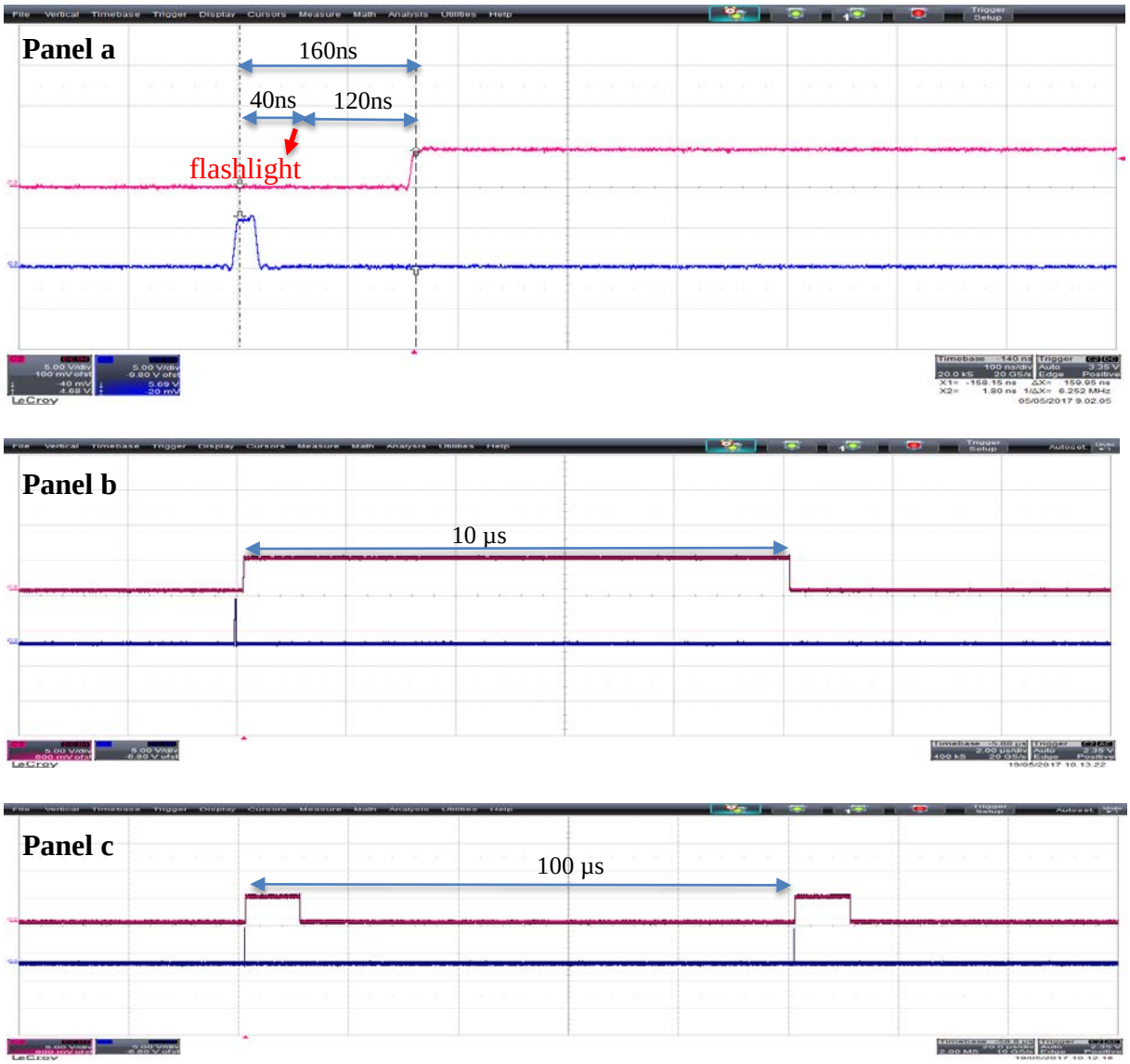

*Figure 11. Panel a) HOLD (red waveform) and TRIGGER (blue waveform). To be noted the total 160ns delay respect to the TRIGGER signal. Additional 40ns are required by the pulsed light sources to be ready for firing. Panel b. The duration of the HOLD signal before to go down is 10*µs, *in fact* we select this for the "Read" signal. *Panel c) The repetition time is 100µs meaning 10 KHz or 10000 pulses/s.*

The amplitude of TRIGGER signal is settled to 3.0V for the pulsed Laser sources while is adjusted in the range 800mV - 6.0V (depending of the source) for the pulsed LED light sources.

3. PDE measurement method with pulsed light source

The PDE measurement is based on the statistical analysis of the pulse heights distribution of the SiPM devices both in light and in the dark conditions.
The used technique was widely discussed in P. Eckert et al., NIMA 620 (2010) 217-226 "Characterization studies of silicon photomultipliers" and in the Hamamatsu document "Technical information MPPC Modules".
The statistical analysis assumes that the number of photons emitted by each impulse (laser and LED) follows the distribution of Poisson:

$$P(\bar{x},x)=\frac{\bar{x}^{x}\, e^{-\bar{x}}}{x!} \quad \text{Density function} \tag{2}$$

Where:
x: Number of detected photons
$\bar{x}$: Mean number of detected photons

In case of absence of photons that means for x = 0 the (2) changes in:

$$P(\bar{x},0)= e^{-\bar{x}} \tag{3}$$

On the other hand, if we indicate with N_{ped} the number of events at 0pe and N_{tot} the total number of events the distribution $P(\bar{x},0)$ is given by the ratio N_{ped}/N_{tot}, that has to be corrected for the presence of the dark expressed by the ratio N_{ped} dark/N_{tot}^{DK}:

$$P(\bar{x},0)= \frac{\frac{N_{ped}}{N_{tot}}}{\frac{N_{ped}^{Dk}}{N_{tot}^{Dk}}} \tag{4}$$

Where:
N_{ped} is the number of events at 0pe (that is the pedestal) with light source.
N_{tot} is the number of the total events with light source**.**
N_{ped}^{DK} is the number of events at 0pe (that is the pedestal) without light source (Dark).
N_{tot}^{DK} is the number of the total events without light source**.**

By equating member-to-member (3) and (4) we obtain:

$$e^{-\bar{x}} = \frac{\frac{N_{ped}}{N_{tot}}}{\frac{N_{ped}^{Dk}}{N_{tot}^{Dk}}} \quad (5)$$

That, applying the logarithm to the two members, turns in:

$$\bar{x} = \bar{N}_{SiPM} = -\ln\left[\frac{\frac{N_{ped}}{N_{tot}}}{\frac{N_{ped}^{Dk}}{N_{tot}^{Dk}}}\right] \quad (6)$$

From which we derive the **average number of photons revealed by SiPM $\bar{N}_{SiPM}$:**

$$\bar{N}_{SiPM} = -\ln\left[\frac{N_{ped}}{N_{tot}}\right] + \ln\left[\frac{N_{ped}^{Dk}}{N_{tot}^{Dk}}\right] \quad (7)$$

If the total number of pulses with light source N_{tot} equals the one without light source (Dark condition) $\mathbf{N_{tot} = N_{tot}^{DK}}$

We have:

$$\bar{N}_{SiPM} = -\ln\left[\frac{N_{ped}}{N_{ped}^{Dk}}\right] \rightarrow \bar{N}_{SiPM} = \ln\left[\frac{N_{ped}^{Dk}}{N_{ped}}\right] \quad (8)$$

Considering the **average number of photons revealed by calibrated photodiode $\bar{N}_{ph\ cal\text{-}Diode}$** and the sensitive areas of both detectors, we can obtain the PDE as:

$$PDE = \frac{\bar{N}_{SiPM}}{\bar{N}_{ph\ Cal\text{-}Diode}} \times \frac{A_{Diode}}{A_{SiPM}} \quad (9)$$

Where:

$$N_{ph\ Cal\text{-}Diode} = \frac{N_e}{QE(\lambda)} \quad (10)$$

With N_e the number of photoelectrons detected by the calibrated photodiode and $QE(\lambda)$ its Quantum Efficiency.

Figure 12 shows a theoretical PHD with and without pulsed light.

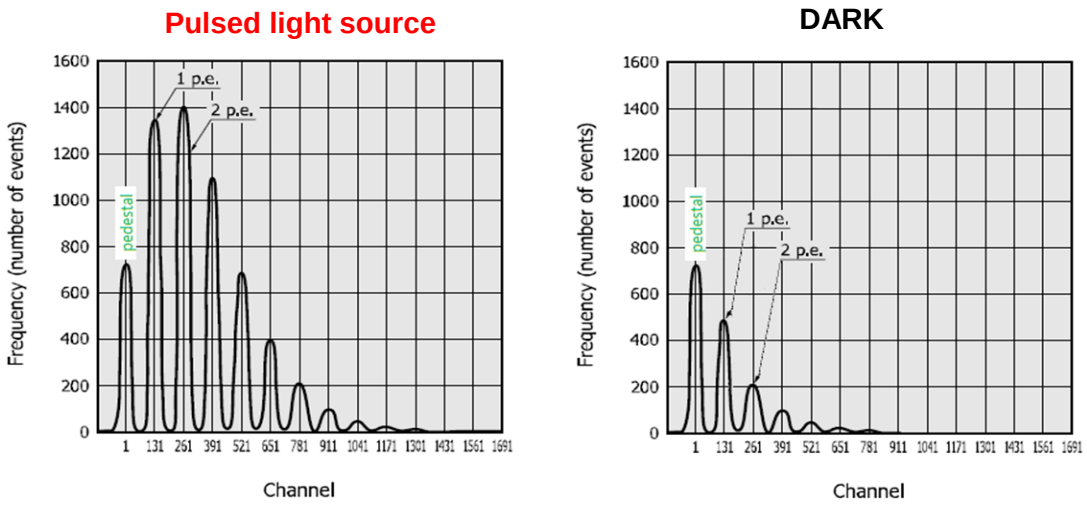

Figure 12. Theoretical Pulse Height Distribution with (left plot) and without (right plot) pulsed light.

The combined plots depicted in Figure 13 show how the dark can influence the PDE measurement.

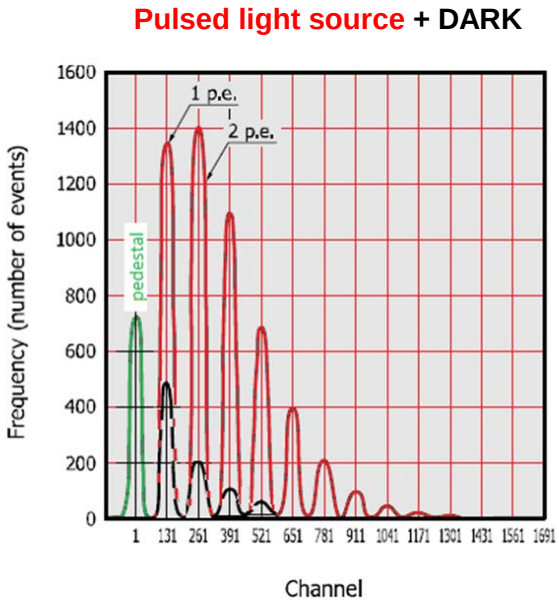

Figure 13. Combined PHD related to the light source and to the dark. To be noted the same position of the pedestal in both cases.

The experimental case is reported in Figure 14 where the PHD plots for the MPPC LCT5 3x3 mm^2,pich size 75µm in both operating conditions are shown. As pulsed light source we used a Laser source with wavelength λ=405nm.

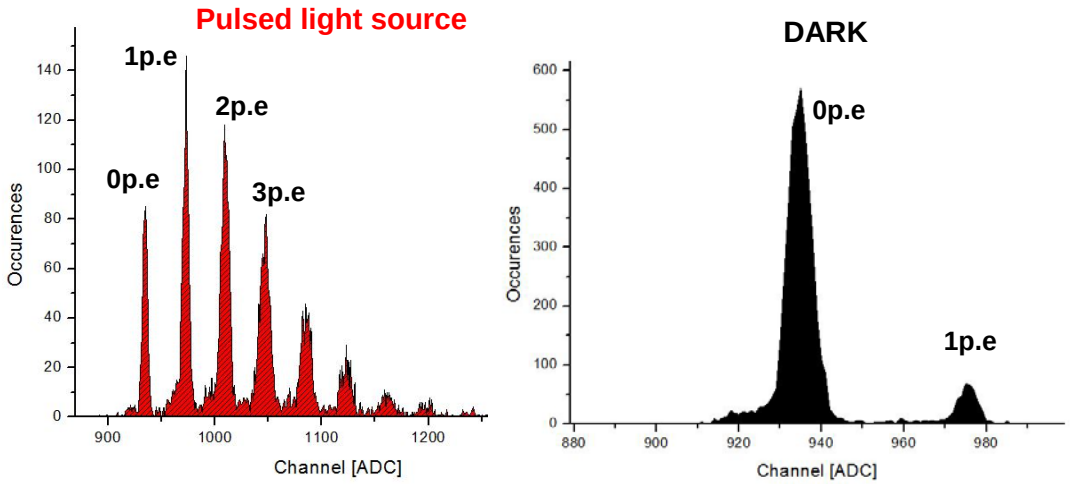

Figure 14. PHD plots for the MPPC LCT5 3x3 mm^2 (micro-cell 75µm) illuminated (left plot) and in dark (right). To be noted the same position 934 ADC of the pedestal in both cases.

As can be noted for each peak of the distribution we have the correspondent ADC value of the level of one photoelectron (1p.e.), two photoelectrons (2p.e.), and so on. The distribution of the occurrences will follow the Poisson law of course. At the base of each peak can be observed an enlargement due to the optical cross talk and after-pulse effects. Only the first peak (pedestal = 0p.e.) is not affected. The distribution corresponding to the 0p.e., named $\mathbf{N_{ped}}$, indicates the number of events due to the signal (either source or dark) not affected by OCT and after pulse because no extra photons are generated by the primary photon.
$\mathbf{N_{ped}}$ and $\mathbf{N_{ped}^{DK}}$ are used to evaluate the **average number of photons revealed by SiPM,** named $\mathbf{\bar{N}_{SiPM}}$, in the formula (7) and thus to evaluate the PDE.

4. Hamamatsu LCT5 and LVR series Detectors Characterization

We carried out the characterization measurements, as stated above, on the Hamamatsu SiPM detectors LCT5, LVR and LVR2 series. The detectors are listed in Table 3.

Table 3. List of characterized SiPM detectors

Device name	Dimensions [mm^2]	Pich size [µm]	Coating	BV @25°C [V]	Gain @3V OV	DCR @6°C [cnts/s]
LCT5 3050CS	3 x 3	50	Silicone	52.50	2.0x10^6	
LCT5 7050CS	7 x 7	50	Silicone	52.80	2.0x10^6	3.41 x10^5
LCT5 3075CS	3 x 3	75	Silicone	51.30	3.3x10^6	
LCT5 6075CS	6 x 6	75	Silicone	52.01	3.3x10^6	2.54 x10^5
LCT5 7075CS	7 x 7	75	Silicone	52.70	3.3x10^6	4.00 x10^5
LVR 3050CS	3 x 3	50	Silicone	36.80	2.8x10^6	
LVR2 3050CN	3 x 3	50	Bare	38.26	2.8x10^6	
LVR2 7050CS	7 x 7	50	Silicone	38.20	2.8x10^6	7.96 x10^5
LVR2 7050CN	7 x 7	50	Bare	38.60	2.8x10^6	6.52 x10^5

Using the set-up of Figure 1, we performed the measurements on the relevant parameters that characterize the detectors. We essentially measured the Optical Cross Talk (OCT) versus the overvoltage OV, the Photon Detection Efficiency (PDE) at the wavelength of 405 nm versus the OV by using the LDH-P-C-405 Laser source from PicoQuant and the PDE in the 350nm – 850nm spectral range by using all the pulsed light sources described in section 2.1.

4.1 Optical Cross-Talk (OCT) measurements

Before discussing the OCT results, we have to introduce two problems:

- The pile-up effect that leads to an underestimation of the DCR and is essentially due to the combination of the SiPM recovery time and the timing of the ASIC electronics. The more microcells are on a SiPM the more pronounced is the pile-up effect.
- Inefficient Zero Pole Cancellation (ZPC) of the High Pass Filter (HPF) (CR input circuit of the Citiroc shaper) that is responsible for the overestimation of the second p.e.

In fact, using the formula (1) discussed in section 2.4.1, if the DCR at 0.5 p.e. is underestimated and the DCR at 1.5 p.e. is overestimated we obtain an OCT overestimated.

Thus, we will have two effects that can give false OCT values:

1. Pile-up effect.
2. Inefficient High Pass Filter → inefficient zero pole cancellation.

In both cases, the OCT will result higher than that effective.

Independently from the above-mentioned effects, the OCT rises with the sensitive area because the probability to have the LED emission effect is directly proportional to the number of microcells. Another important parameter that play an important role in OCT performance is the presence of the protective coating on top of the sensitive surface. In other words if the pile-up and the inefficient ZPC effects are neglected, the OCT will be higher for SiPMs with higher dimensions and with s ilicone coating.

While the second effect is impossible to remove or adjust because the derivative circuit is inside the ASIC chip, the first effect can be mitigated because depends on the count rate. Lowering the temperature the DCR will fall down and thus the pile-up probability will decrease. We have investigated the pile-up effect on the bare devices LVR2 3050 CN, LVR2 6050 CN and LVR2 7050 CN by measuring the OCT at 3V of OV as function of the temperature or, in turn, as function of the DCR. The result is shown in Figure 15.

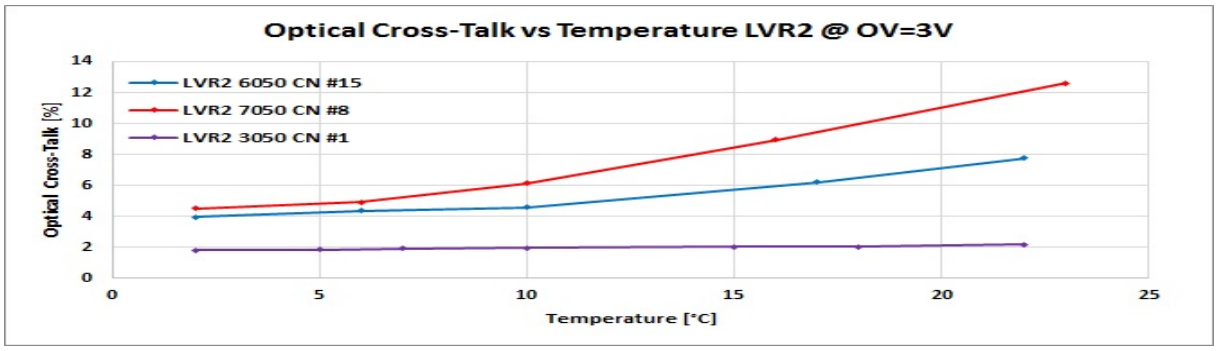

Figure 15. OCT versus temperature for the bare devices LVR2 3050 CN, LVR2 6050 CN and LVR2 7050 CN).

As can be noted for temperatures below 6°C, the LVR2 6050 CN shows an OCT around 4%, the LVR2 7050 CN shows an OCT around 5%, while the LVR2 3050 CN, being a device of small size, shows an OCT of 2% at any temperature. It seems also that below 6°C the pile-up effect does not influence the OCT measurement for the large detectors and the difference (about 1%) is only due to the different dimensions. Figure 16 depicts the two different behaviors of the devices at temperatures below and above about 6°C. Below 6°C the OCT depends only by the SiPM size while above 6°C the OCT is affected by the pile-up effect.

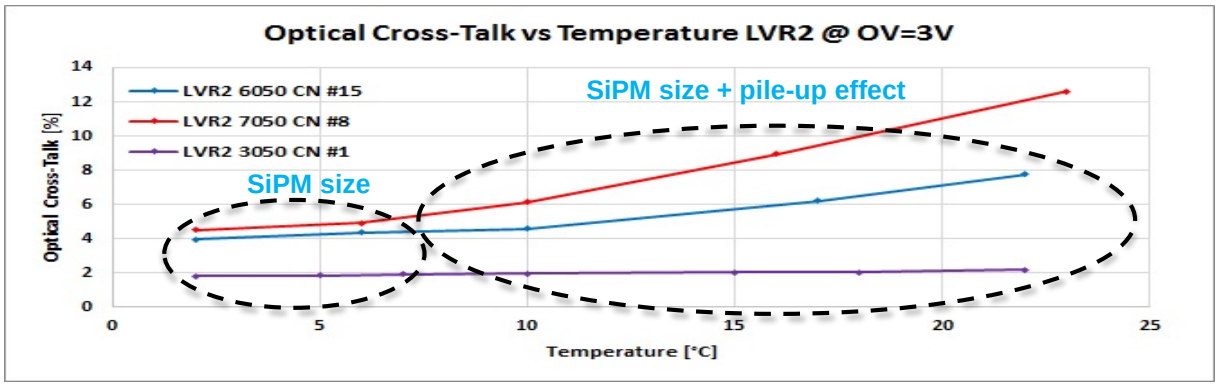

Figure 16. OCT versus temperature. Below 6°C, the OCT depends only by the SiPM size while above 6°C the OCT is affected by the pile-up effect.

4.1.1 OCT versus Overvoltage for the LCT5 Series

The OCT is function of the SiPM operating voltage, or better to say of the applied overvoltage respect to the breakdown voltage. We carried out the OCT measurements at over voltages ranging from 2V to 6V (step 1V).

The obtained results are subdivided by technology (LCT5 or LVR). Figure 17 shows the OCT plots of the 3x3mm^2 LCT5 devices with 50 µm microcells (left) and 75 µm microcells (right). Figure 18 shows the OCT plot of the 6x6mm^2 LCT5 MPPC with 75 µm microcells. Figure 19 shows the OCT plots of the 7x7mm^2 LCT5 devices with 50 µm microcells (left) and 75 µm microcells (right).

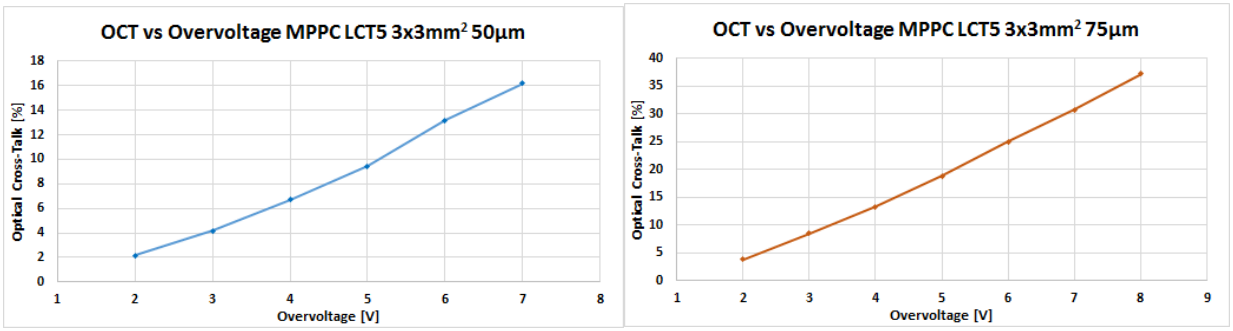

Figure 17. Optical Cross-Talk versus Overvoltage for 3x3 mm^2 LCT5 devices with 50µm microcells (left) and 75µm microcells (right).

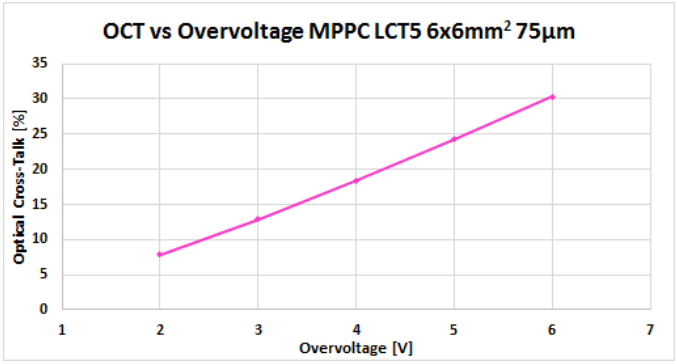

Figure 18. Optical Cross-Talk versus Overvoltage for the 6x6mm^2 LCT5 SiPM with 75 µm microcells

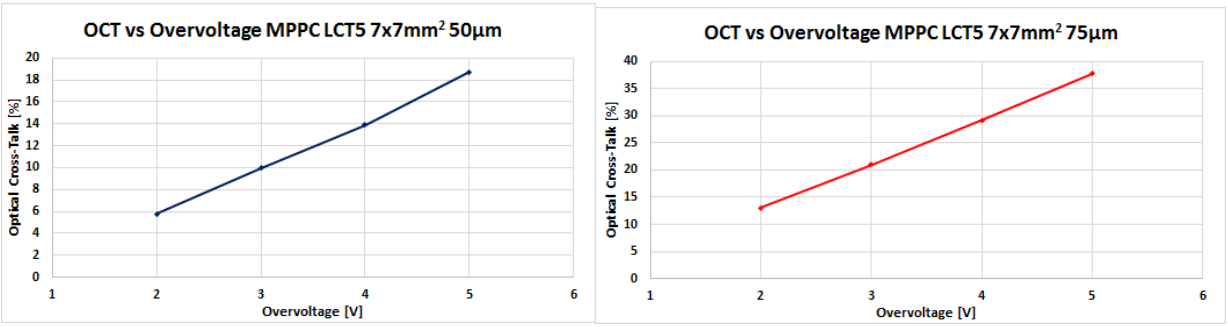

Figure 19. Optical Cross-Talk versus Overvoltage for SiPM LCT5 7x7 mm² LCT5 devices with 50µm microcells (left) and 75µm microcells (right).

We compared all the LCT5 devices in Figure 20.

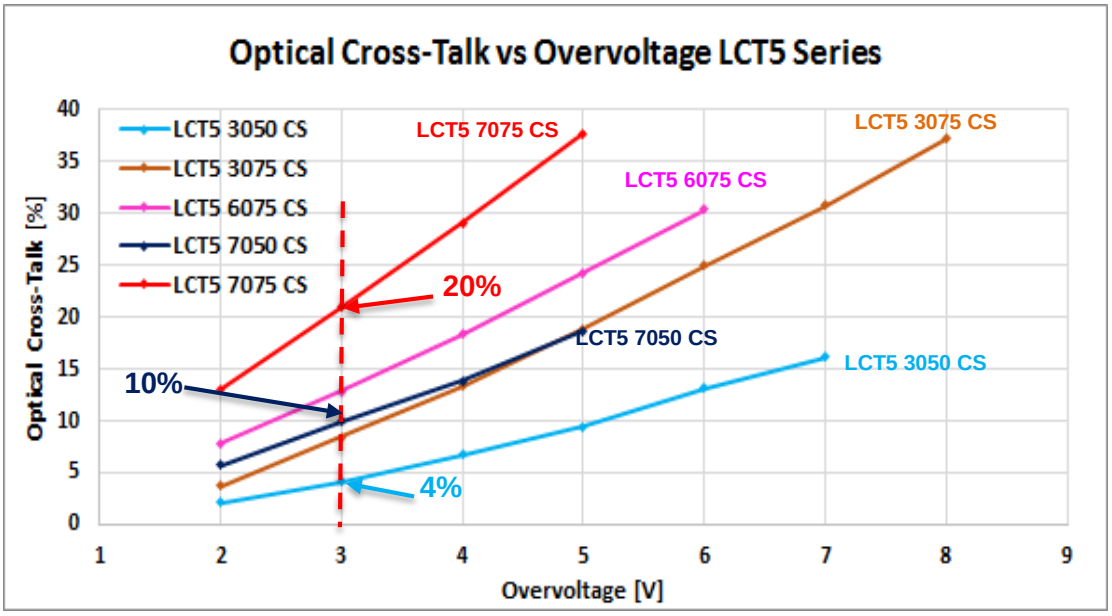

Figure 20. Optical Cross-Talk versus Overvoltage for all the SiPMs LCT5 series.

As expected, the OCT rises with the SiPM dimension: small devices present a lower OCT respect to the larger ones.

At 3 V of overvoltage the LCT5 3x3mm² MPPC with 50µm microcells has about 4% of OCT while at the same over voltage the LCT5 7x7mm² MPPC with 50µm microcells has about 10%, and the LCT5 7x7mm² MPPC with 75µm microcells has about 20%.

At the moment of writing this document the LCT5 7x7mm² MPPCs with both 50µm and 75µm microcells are mounted in the focal plane of the ASTRI camera.

4.1.2 OCT versus Overvoltage for the LVR and LVR2 Series

Hamamatsu has manufactured two LVR types: the LVR and the LVR2 and has decided to produce also uncoated SiPMs (CN series) in order to lower the OCT due to the back reflection on the coating. The MPPC coated with the Silicone protective resin have the name CS at the end of the identifier model. Figure 21 shows the OCT plots of the 3x3mm^2 with 50 µm microcells LVR –CS (left panel) and LVR2 -CN (right panel). Figure 22 shows the OCT plots of the 7x7mm^2 LVR2 devices with 50 µm microcells with Silicone Coating -CS (left) and with No Coating -CN (right).

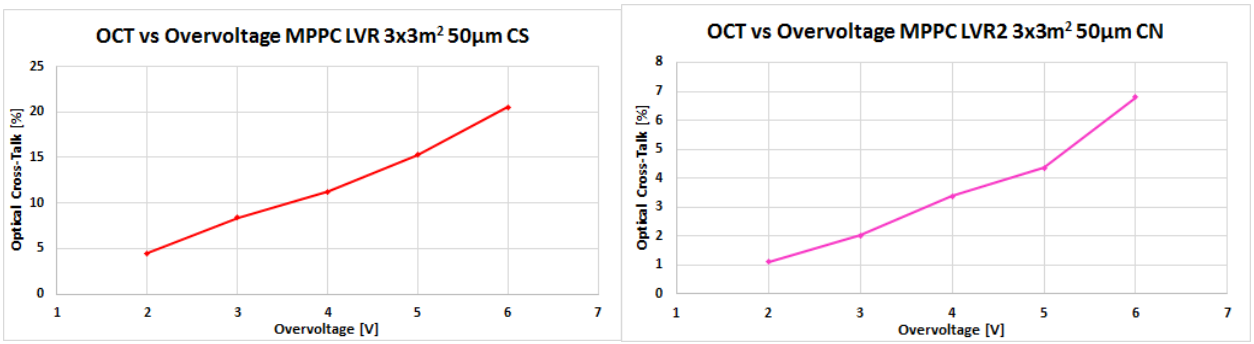

Figure 21. Optical Cross-Talk versus Overvoltage for SiPM LVR 3x3 mm^2 50µm CS and LVR2 3x3 mm^2 50µm CN

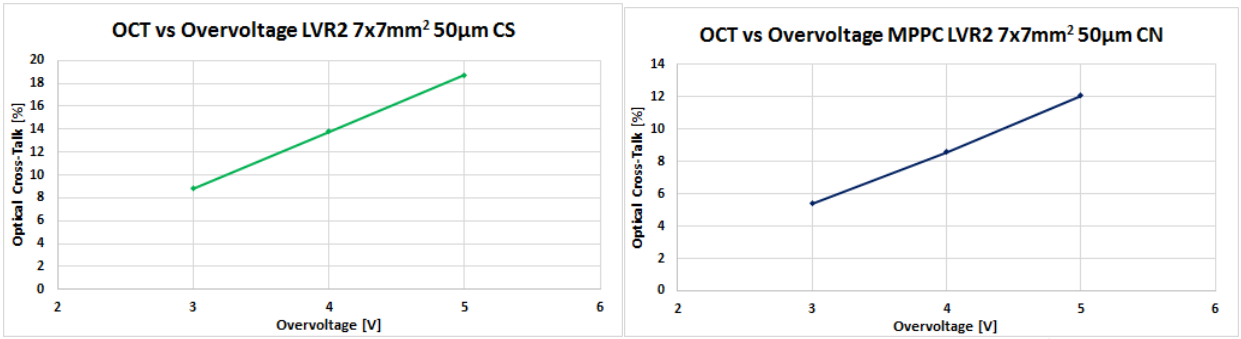

Figure 22. Optical Cross-Talk versus Overvoltage for the SiPMs LVR2 7x7 mm^2 50 µm CS and LVR2 7x7 mm^2 50 µm CN

We compared all the LVR devices in terms of OCT versus Overvoltage in Figure 23.

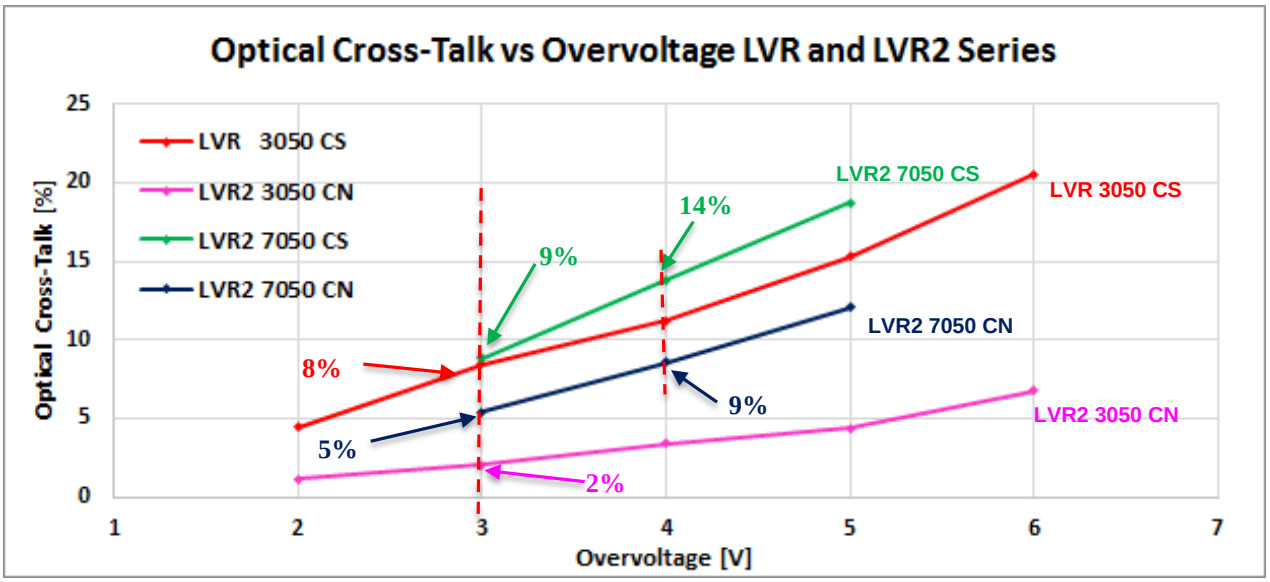

Figure 23. Optical Cross-Talk versus Overvoltage for all the SiPMs LVR series

We observe the same behavior for the LVR devices: the OCT rises with the SiPM dimension.

At 3 V of overvoltage the LVR2 3x3mm^2 MPPC with 50µm microcells shows a surprising OCT of about 2% while at the same over voltage the LVR 3x3mm^2 MPPC with 50µm microcells shows an OCT of 8%. This is due to the different technology between the LVR and LVR2 and to the coating. The LVR2 7x7mm^2 MPPCs show a difference of 4% of OCT between the coated CS and the bare CN.

The difference in OCT rises with the Overvoltage: at 4V of OV the LVR2 7050-CS has an OCT of 14% while the LVR2 7050-CN has an OCT of about 9%. This difference is only due to the presence of the coating on top of the sensitive surface.

Thus, the LVR2 7x7mm^2 bare device seems to be the real candidate for the ASTRI MINI-ARRAY focal plane camera.

4.1.3 OCT versus OV for the 7X7 mm^2 LCT5 and LVR2: Comparison

We reported the comparison between the two technologies for the 7x7mm^2 devices in Figure 24.

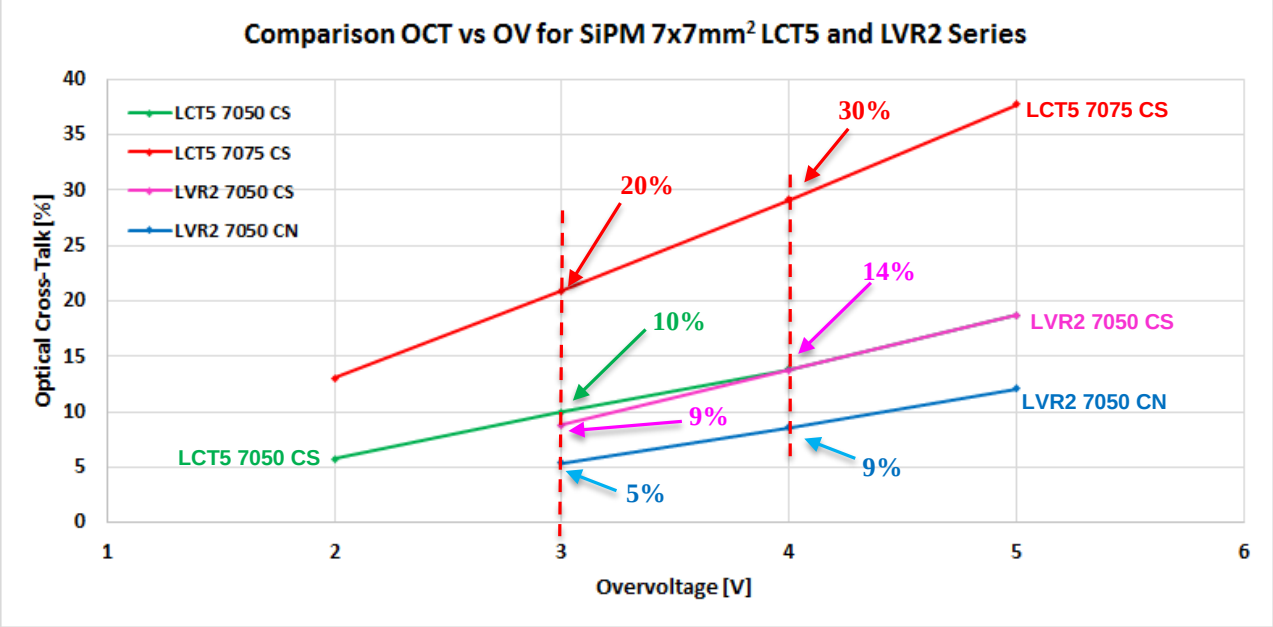

Figure 24. Optical Cross-Talk versus Overvoltage for the 7x7mm^2 *SiPMs comparison between the LCT5 and LVR2 technology. As can be noted the LCT5 with 75µm microcells has an OCT of 20% at 3V of OV while the LCT5 with 50µm microcells at the same OV has an OCT of 10%. This last is comparable to the LVR2 Silicone Coated, but the PDE, as can be seen later, is lower. The effective improvement between the two technologies can be noted at 4V of OV, where the LCT5 has an OCT of 30% while the LVR2 CN has an OCT of only 9%.*

As can be noted from Figure 24 the LCT5 with 75µm microcells has an OCT of 20% at 3V of OV while the LCT5 with 50µm microcells at the same OV has an OCT of 10%. This last is comparable to the LVR2 Silicone Coated, but the PDE, as discussed in the next section, is lower in the case of LCT5. The effective improvement between the two technologies is exploited at 4V of OV, where the LCT5 with 75µm microcells has an OCT of 30% while the LVR2 -CN has an OCT of only 9%. As known at 4V of OV the PDE rises in both cases but the OCT is considerably lower for the LVR2 –CN SiPM.

4.2 Photon Detection Efficiency (PDE) at the wavelength λ=405 nm

Through the set-up described in section 2, the Photon Detection Efficiency (PDE) of all the SiPM devices was measured utilizing a 405nm pulsed laser source and varying the SiPM overvoltage from 2V to 9V at 1V step. In the following sections, the plots relative to the various SiPMs are presented. In the same manner as for the OCT we subdivided the PDE results by technology (LCT5 or LVR).

4.2.1 PDE at λ=405nm for the LCT5 Series MPPC

Figure 25 shows the PDE at λ=405nm plots of the 3x3mm^2 LCT5 devices with 50 µm microcells (left) and 75 µm microcells (right)

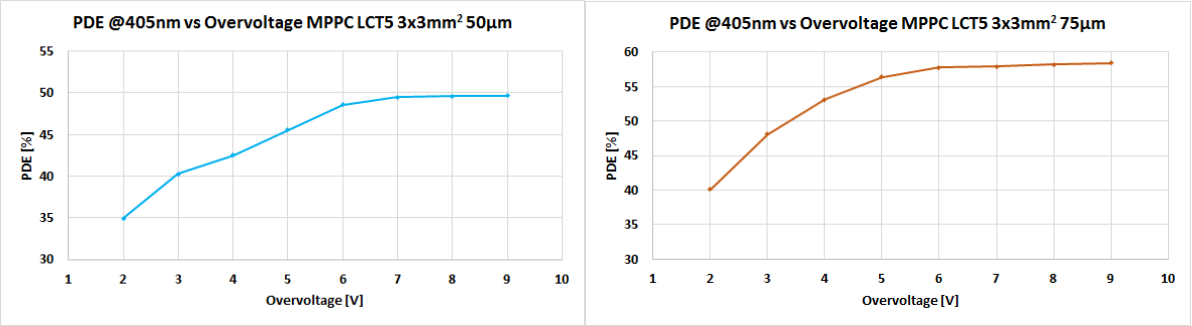

Figure 25. PDE @405nm versus Overvoltage of the LCT5 3x3 mm^2 50µm and 75µm SiPMs

The PDE@405nm saturates at 6V of Overvoltage for both devices and is about 50% for the LCT5 3x3 mm^2 50µm while reaches about 58% in the LCT5 3x3 mm^2 75µm case.

Figure 26 shows the PDE@405nm plot of the 6x6 mm^2 LCT5 MPPC with 75 µm microcells.

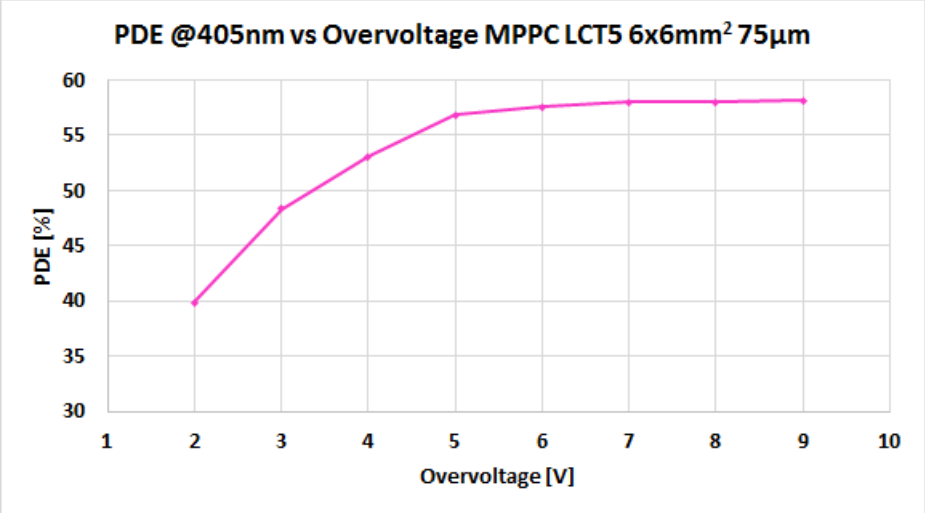

Figure 26. PDE @405nm versus Overvoltage for SiPM LCT5 6x6 mm^2 75µm

The PDE@405nm, as for the 6x6 mm^2 75µm microcells, saturates at 6V of Overvoltage and reaches about 58%.

Figure 27 shows the PDE@405nm plots of the 7x7mm^2 LCT5 devices with 50µm microcells (left) and 75µm microcells (right).

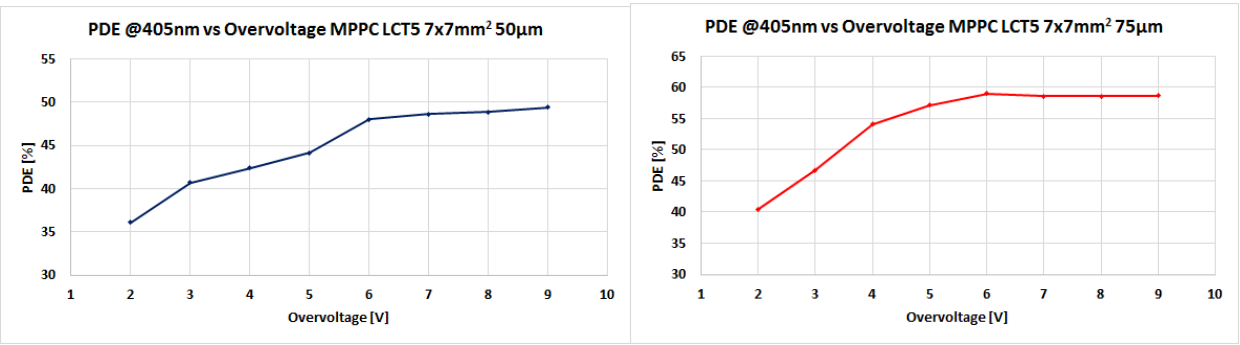

Figure 27. PDE @405nm versus Overvoltage for SiPM LCT5 7x7 mm^2 50µm (left panel) and 75µm (right panel).

The PDE@405nm, as for the other LCT5 devices, saturates at 6V of Overvoltage and shows the same behavior.

In Figure 28, we report the conclusive plot that compares the LCT5 family devices in terms of PDE@405nm vs OV.

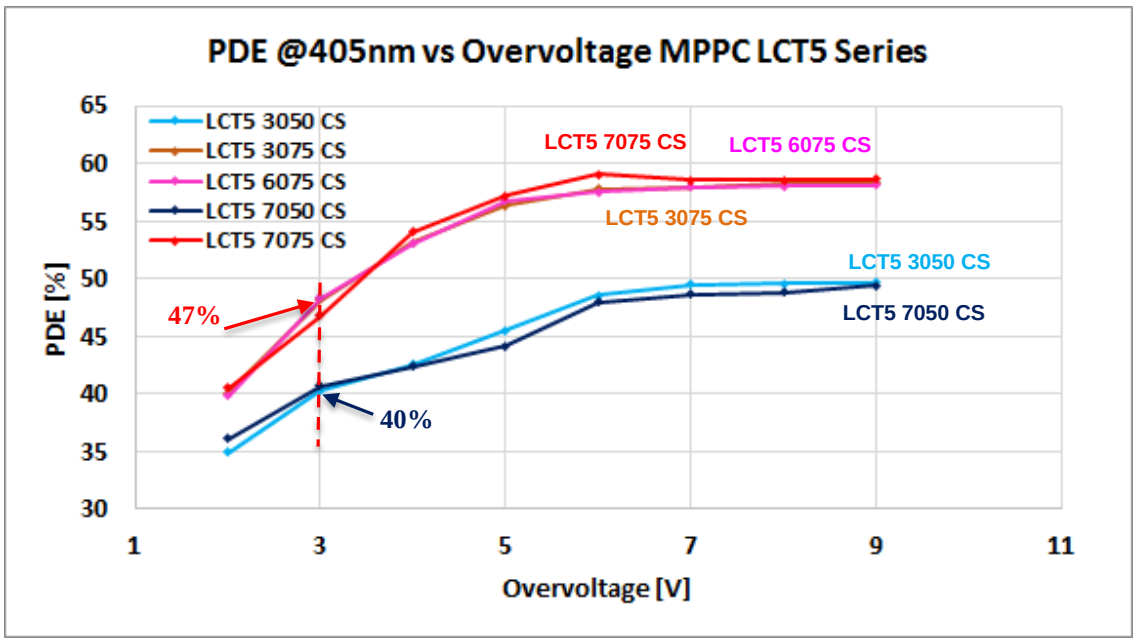

Figure 28. PDE @405nm versus Overvoltage for the LCT5 SiPM series.

As expected, the PDE does not depend from the dimensions but only by microcells. The measured PDE@405nm at the saturation level is about 60% for75µm microcells case while is about 50% for 50µm microcells case.

At 3V of overvoltage The LCT5 with 50µm show a PDE@405nm of 40% while the LCT5 with 75µm show a PDE@405nm of about 47%.

4.2.2 PDE at λ=405nm for the LVR and LVR2 Series MPPC

Figure 29 shows the PDE at λ=405nm plots of the 3x3mm^2 LVR devices with 50 µm microcells LVR with Silicone Coating -CS (left) and LVR2 Not Coated -NC (right).

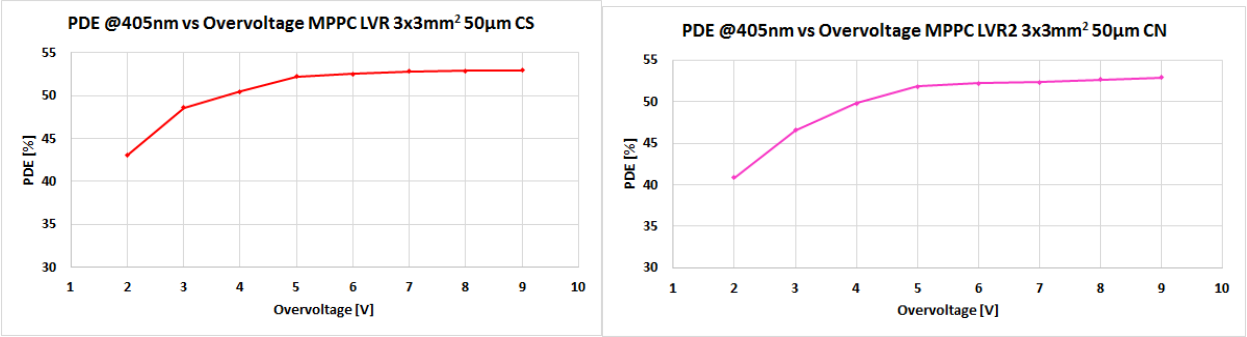

Figure 29. PDE @405nm versus Overvoltage for 3x3 mm^2 SiPM with 50µm microcells LVR -CS (left panel) and LVR2 –CN (right panel).

The PDE@405nm for the LVR devices saturates at 5V instead of the 6V of Overvoltage as for the LCT5 case and is about 53%.

Figure 30 shows the PDE at λ=405nm plots of the 7x7mm^2 LVR2 devices with 50 µm microcells LVR with Silicone Coating -CS (left) and Not Coated -NC (right).

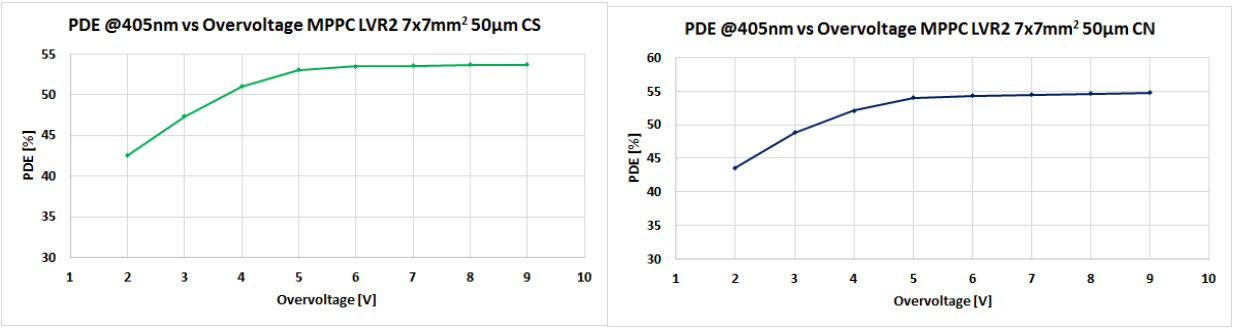

Figure 30. PDE @405nm versus Overvoltage for LVR2 7x7 mm^2 50 µm SiPMs Silicone Coated -CS (left panel) and Not Coated –CN (right panel).

As expected the PDE@405nm, as for the for the other LVR devices, saturates at 5V of Overvoltage and shows the same behavior.

In Figure 31, we report the conclusive plot that compares the LVR family devices in terms of PDE@405nm vs OV.

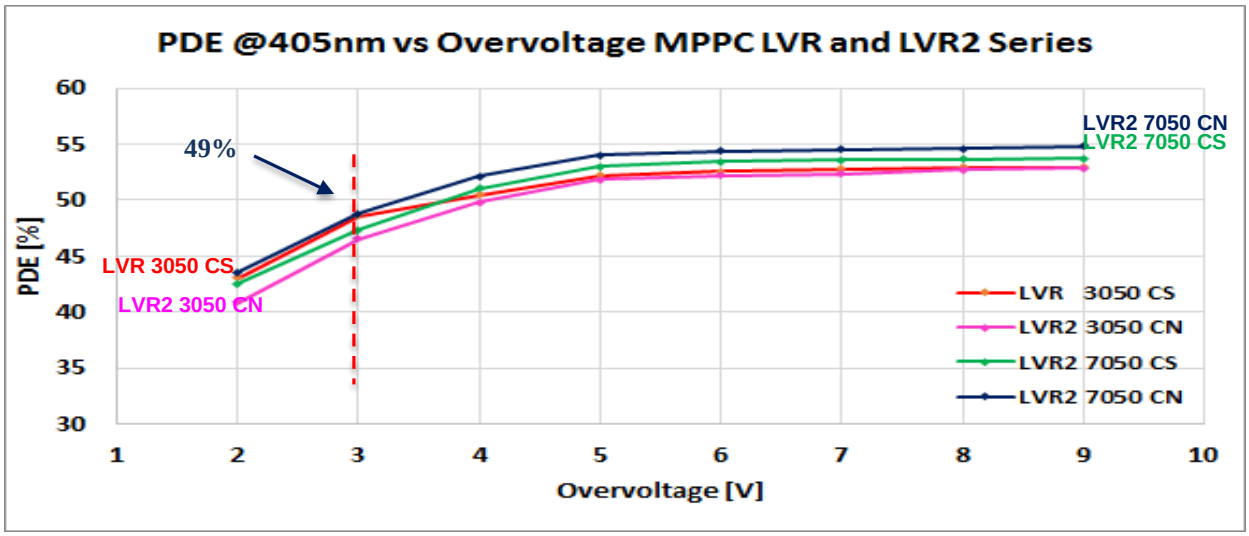

Figure 31. PDE @405nm versus Overvoltage for the LVR and LVR2 Silicone Coated -CS and No Coating -CN

The measured PDE@405nm at the saturation level obtained at 5V of overvoltage is about 55%

At 3V of overvoltage, we can affirm that the LVR family with 50µm microcells show a PDE@405nm of 49% near to that of the LCT5 with 75µm microcells. Thus, the parameter that make the difference is the OCT. The difference between the two families can be evaluated in section 4.2.4 were we report the PDE versus the OCT for all the characterized devices.

4.2.3 PDE at 405nm vs OV for 7x7 mm^2 LCT5 and LVR2: Comparison

In Figure 32, we report the conclusive plot that compares the 7x7mm^2 LCT5 and LVR2 family devices in terms of PDE@405nm vs OV.

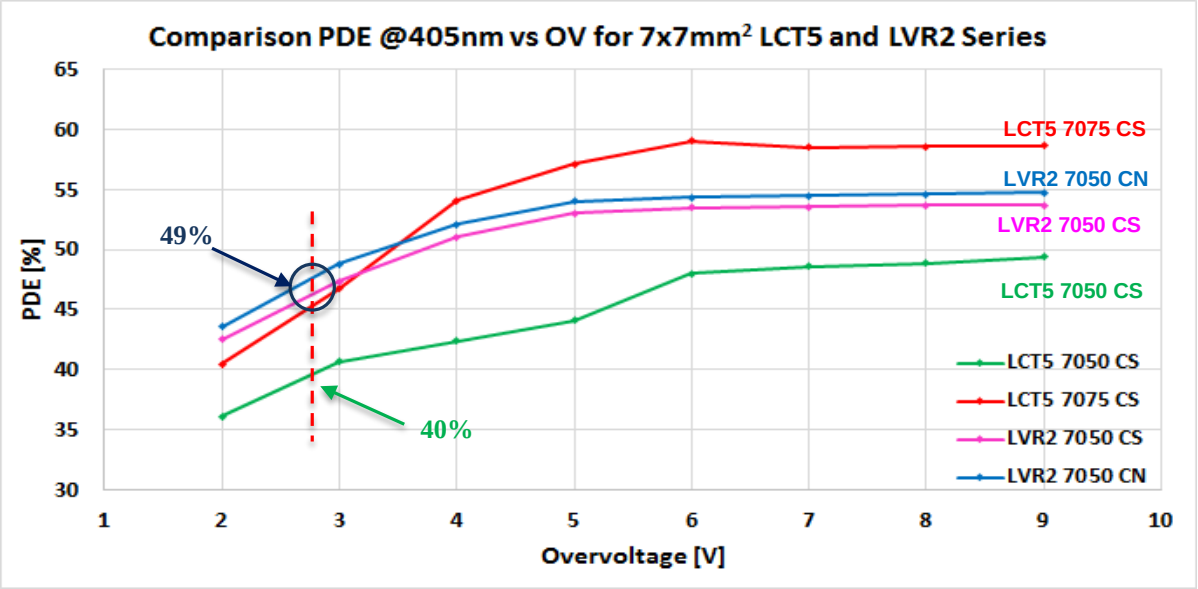

Figure 32. PDE @405nm versus Overvoltage for the 7x7mm^2 *LCT5 and LVR2 family devices.*

As stated above, the PDE at 405nm of the LCT5 with 75µm microcells is smilar to that of the LVR2 with 50µm microcells. While the LCT5 with 50µm microcells at the same overvoltage is about 9% less.

4.2.4 PDE at 405nm vs OCT for 7x7 mm^2 LCT5 and LVR2: Comparison

In Figure 33, we report the plot that compares the 7x7mm^2 LCT5 and LVR2 family devices in terms of PDE@405nm versus OCT.

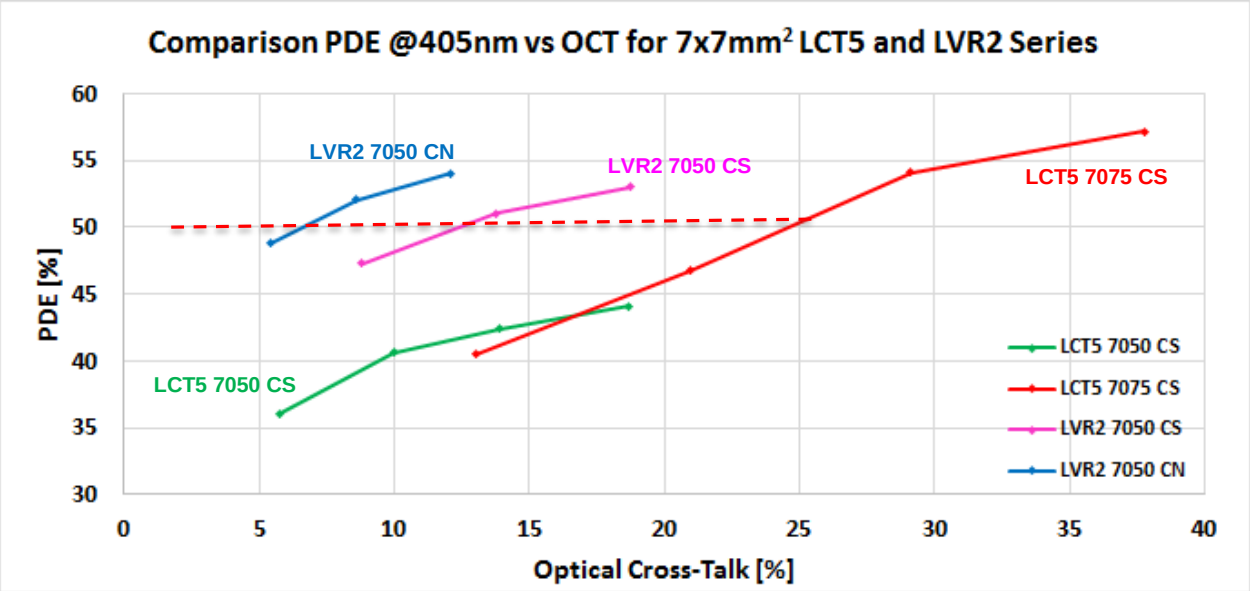

Figure 33. PDE @405nm versus Optical Cross Talk for the 7x7mm^2 *LCT5 and LVR2 family devices.*

As can be noted from the plot, to have a **50% of PDE at 405nm** we have to operate:

- the SiPM **LVR2 7050-CN** with an overvoltage of 3.2 V obtaining an OCT of **6%**
- the SiPM **LVR2 7050-CS** with an overvoltage of 3.7 V obtaining an OCT of **13%**
- the **SiPM LCT5 7075-CS** with an overvoltage of 3.5 V obtaining an OCT of **25%**

The LCT5 7050-CS is unable to obtain PDE higher than 44%.

4.3 PDE in the 300 – 850nm spectral range for the LCT5 and LVR2 series

The Photon Detection Efficiency in the 300 – 850 nm wavelength range of all the SiPM devices has been measured at 3V of overvoltage and utilizing the same set-up described in section 2. In this case, we used all the pulsed laser sources listed in Table1. We measured the PDE for the LCT5 3075-CS, the LVR 3050-CS and the LVR2 3050-CN that are representative of the technologies adopted by Hamamatsu. We compared the results in the next section.

Figure 34 shows the PDE in the 300 – 850 nm spectral range for the 3x3mm^2 LCT5 SiPM with 75µm microcells and Silicone coated (CS).

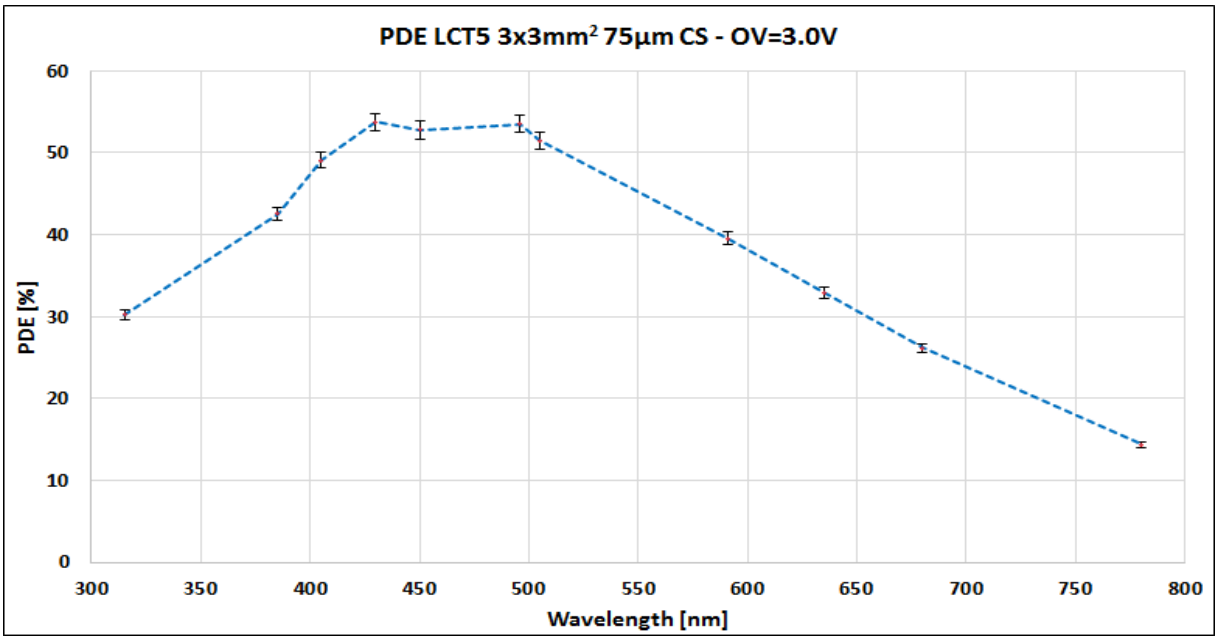

Figure 34. PDE in the 300 – 850 nm spectral range for the 3x3mm^2 LCT5 SiPM with 75µm microcells.

As can be noted the PDE is higher than 30% at wavelength 300-350 nm, at 385nm the PDE is higher than 40% and peaks at 53% in the 430 – 490 nm interval.

Figure 35 shows the PDE in the 300 – 850 nm spectral range for the 3x3mm^2 LVR SiPM with 50µm microcells and Silicone coated (CS).

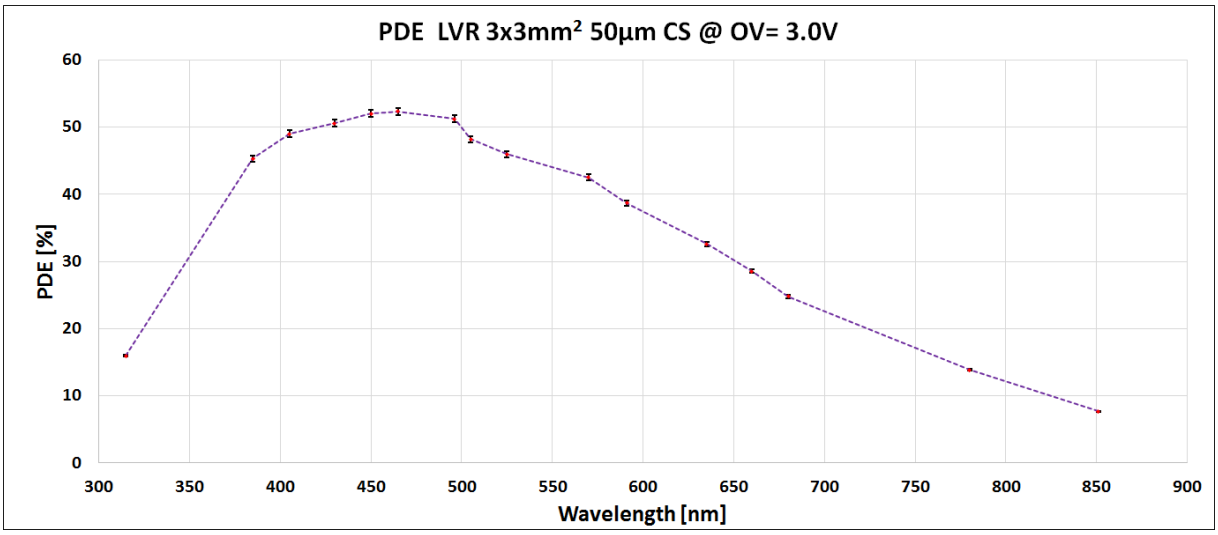

Figure 35. PDE in the 300 – 850 nm spectral range for the 3x3mm^2 LVR SiPM with 50µm microcells.

In this case, the PDE at 385nm the PDE is higher than 45% and peaks at 51% in the 430 – 490 nm interval.

Figure 36 shows the PDE in the 300 – 850 nm spectral range for the 3x3mm^2 LVR2 SiPM with 50µm microcells without coating (NC).

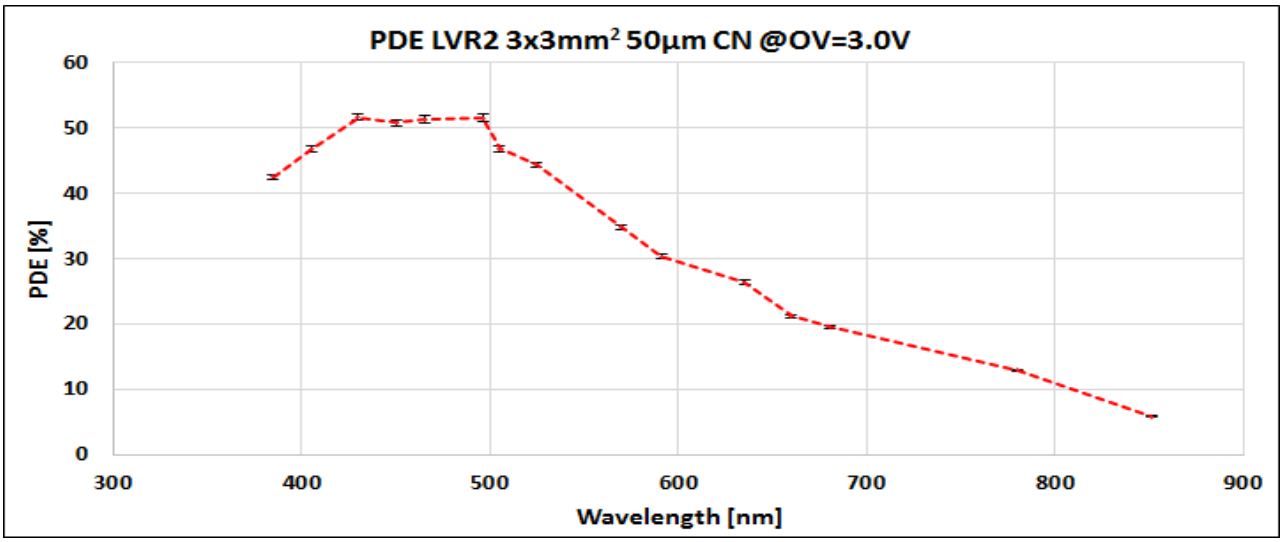

Figure 36. PDE in the 300 – 850 nm spectral range for the 3x3mm^2 LVR2 SiPM with 50µm microcells with no coating (NC).

In this case, the PDE at 385nm the PDE is higher than 40% and peaks at 51% in the 430 – 490 nm interval.

4.3.1 PDE in the 300 – 850nm range: Comparison LCT5, LVR and LVR2 series

In Figure 37, we report the plot that compare the PDE in the 300-850 nm of LCT5 with 75µm microcells, LVR and LVR2 with 50µm, microcells devices.

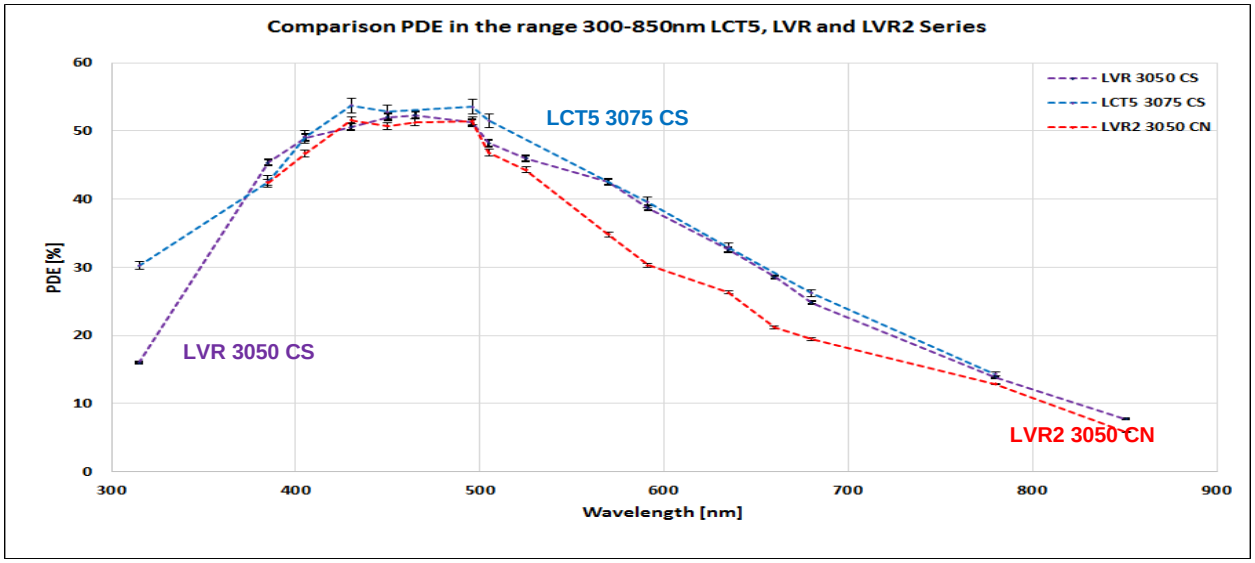

Figure 37. PDE in the 300 – 850 nm spectral range comparison for the LCT5 with 75µm microcells and LVR2 with 50µm microcells with no coating (NC) SiPMs.

As can be noted from the PDE plots the three devices shows a similar behavior in the peak spectral interval (430nm – 500 nm), in fact at 3V of overvoltage the PDE is around 52%. Instead, an interesting and relevant improvement from the point of view of the Cherenkov light is the lower PDE at wavelength higher than 550nm showed by the LVR2 technology respect to the other two technologies.

5. Conclusions

As stated above this work is intended at the selection of the most suitable detectors to cover the ASTRI-Mini Array telescopes focal plane. The characterization results are condensed in Table 4 where are reported the 7x7 mm^2 devices manufactured by Hamamatsu with different microcells and different technology. The relevant parameters that drive the selection are essentially the PDE at 3V or 4V of overvoltage and the correspondent Optical Cross Talk.

Table 4. List of characterized SiPM detectors

Device name	OV [V]	Pitch size [µm]	PDE @405nm [%]	PDE @ 430-500 nm [%]	OCT [%]
LCT5 7050CS	3	50	41	49	10
	4	50	43	-	14
LCT5 7075CS	3	75	47	53	20
	4	75	54	57	30
LVR2 7050CS	3	50	47	52	9
	4	50	51	56	14
LVR2 7050CN	3	50	49	52	5
	4	50	52	56	9

As ca be derived from Table 4, the LCT5 with 75µm technology shows a very good PDE of 54% at an overvoltage of 3V and even better near 57% at 4V of overvoltage. Unfortunately, for this kind of device, an OCT of 20% at 3V of OV and an unacceptable OCT of 30% at 4V of OV is found. Instead, a good candidate for our application is the **LVR2 7050CN** operated at **4V of overvoltage**.

At these operating conditions, we can have

- A **PDE** peak in the wavelength range 430nm – 500nm of **56%**
- An **OCT** of only **9%.**

All files related to the experimental measurements presented in this report, are located in the database on the PC-LAB (COLD) site Astrophysical Observatory of Catania, path C:\Users\CCDLab1\Desktop\Romeo\Misure

6. CONTACTS

The team working on the electronic design of the ASTRI camera is composed by people from INAF's Catania Astrophysical Observatory and Palermo IFC. It is also referred to as the Electronics Camera Team.

Giovanni Bonanno	giovanni.bonanno@oact.inaf.it	OACT Catania
Giuseppe Romeo	giuseppe.romeo@oact.inaf.it	OACT Catania
Alessandro Grillo	alessandro.grillo@oact.inaf.it	OACT Catania
Salvatore Garozzo	sgarozzo@oact.inaf.it	OACT Catania
Davide Marano	dmarano@oact.inaf.it	OACT Catania
Osvaldo Catalano	osvaldo.catalano@iasf-palermo.inaf.it	IFC Palermo
Giovanni La Rosa	larosa@ifc.inaf.it	IFC Palermo
Giuseppe Sottile	sottile@ifc.inaf.it	IFC Palermo
Salvatore Giarrusso	jerry@ifc.inaf.it	IFC Palermo
Domenico Impiombato	domenico.impiombato@ifc.inaf.it	IFC Palermo